



VILNIUS GEDIMINAS TECHNICAL UNIVERSITY
FACULTY OF MECHANICS
DEPARTMENT OF MECHANICS AND MATERIALS ENGINEERING

Vilius Kavaliauskas

**INVESTIGATION OF DYNAMIC PROCESSES OF PRECISION
POSITIONING SYSTEMS WITH LINEAR MOTOR**
**PRECIZINIŲ POZICIONAVIMO SISTEMŲ SU TIESINIŲ VARIKLIŲ
DINAMINIŲ PROCESŲ TYRIMAI**

Master's degree Thesis

Mechanical engineering study programme, state code 6211EX047

Design and Production of Mechanical Systems specialisation

Mechanical Engineering study field

Vilnius, 2021

VILNIUS GEDIMINAS TECHNICAL UNIVERSITY
FACULTY OF MECHANICS
DEPARTMENT OF MECHANICS AND MATERIALS ENGINEERING

APPROVED BY
Head of Department

(Signature)

(Name, Surname)

(Date)

Vilius Kavaliauskas

**INVESTIGATION OF DYNAMIC PROCESSES OF PRECISION
POSITIONING SYSTEMS WITH LINEAR MOTOR**

**PRECIZINIŲ POZICIONAVIMO SISTEMŲ SU TIESINIŲ VARIKLIŲ
DINAMINIŲ PROCESŲ TYRIMAI**

Master's degree Thesis

Mechanical engineering study programme, state code 6211EX047

Design and Production of Mechanical Systems specialisation

Mechanical Engineering study field

Supervisor doc. dr. Algirdas Maknickas _____
(Title, Name, Surname) (Signature) (Date)

Consultant doc. dr. Artūras Kilikevičius _____
(Title, Name, Surname) (Signature) (Date)

Consultant _____
(Title, Name, Surname) (Signature) (Date)

Vilnius, 2021

VILNIUS GEDIMINAS TECHNICAL UNIVERSITY
FACULTY OF MECHANICS
DEPARTMENT OF MECHANICAL AND MATERIAL ENGINEERING

Mechanical Engineering study field
Mechanical Engineering study programme, state code 6211EX047
Design and Production of Mechanical Systems

APPROVED BY
Head of Department



(Signature)
Mindaugas Jurevičius
(Name, Surname)
2020-01-28

(Date)

OBJECTIVES FOR MASTER'S DEGREE FINAL WORK

.....No.
Vilnius

For student Vilius Kavaliauskas
(Student's Name, Surname)

Final work (project) title: „Investigation of Dynamic Processes of Precision Positioning Systems with Linear Motor“
„Precizinių pozicionavimo sistemų su tiesiniu varikliu dinaminių procesų tyrimai“

Approved on 22th of November, 2019 by Dean's decree No. 224me
(day, Month) (year)

The Final work has to be completed by 18th of May 2021
(Day, Month) (Year)

THE OBJECTIVES:

Introduction.

Literature review.

Analytical investigation of dynamic processes of precision positioning systems with linear motor.

Experimental investigation of dynamic processes of precision positioning systems with linear motor.

Analysis and comparison of the analytical and experimental results.

Conclusions.

List of References.

Consultants of the final degree work:

.....
.....
Academic Supervisor
(Signature) (Title, Name, Surname)
doc. dr. Artūras Kilikevičius
(Title, Name, Surname)

Objectives accepted as a guidance for my Final work

.....
(Student's signature)
Vilius Kavaliauskas
(Student's Name, Surname)
2020-01-28
(Date)

(Baigiamojo darbo sąžiningumo deklaracijos forma)

VILNIAUS GEDIMINO TECHNIKOS UNIVERSITETAS

Vilius Kavaliauskas, 20153541

(Studento vardas ir pavardė, studento pažymėjimo Nr.)

Mechanikos fakultetas

(Fakultetas)

Mechanikos inžinerija, MSGfmu-19

(Studijų programa, akademinė grupė)

BAIGIAMOJO DARBO (PROJEKTO)

SĄŽININGUMO DEKLARACIJA

2021 m. gegužės 19 d.

Patvirtinu, kad mano baigiamasis darbas tema „Precizinių pozicionavimo sistemų su tiesiniu varikliu dinaminių procesų tyrimai“ patvirtintas 2019 m. lapkričio 22 d. dekanu potvarkiu Nr. 224me, yra savarankiškai parašytas. Šiame darbe pateikta medžiaga nėra plagijuota. Tiesiogiai ar netiesiogiai panaudotos kitų šaltinių citatos pažymėtos literatūros nuorodose.

Prenkant ir įvertinant medžiagą bei rengiant baigiamąjį darbą, mane konsultavo mokslininkai ir specialistai: docentas daktaras Algirdas Maknickas. Mano darbo vadovas docentas daktaras Algirdas Maknickas.

Kitų asmenų indėlio į parengtą baigiamąjį darbą nėra. Jokių įstatymų nenumatytų piniginių sumų už šį darbą niekam nesu mokėjęs (-usi).

(Parašas)

Vilius Kavaliauskas
(Vardas ir pavardė)

Vilnius Gediminas Technical University
Faculty of Mechanics
Department of Mechanical and Material Engineering

ISBN ISSN
Copies No.
Date-.....-.....

Master Degree Studies **Mechanical Engineering** study programme Master Graduation Thesis 4

Title **Investigation of Dynamic Processes of Precision Positioning Systems with Linear Motor**

Author **Vilius Kavaliauskas**

Academic supervisor **Algirdas Maknickas**

Thesis language: English

Annotation

Fast-paced competition in industrial environment require high accuracy and performance systems, which allow the industry players to stay on top. The change in mechanical structure of the precision positioning system is no longer enough. Therefore, frequency domain analysis must be done.

In master thesis, theoretical analysis of precision positioning systems with linear motors were done, with theoretical modal analysis of research object, using "SolidWorks" software package. Experiment setup was made, and dynamic analysis and optimization of linear translation stage was performed.

Structure: introduction, literature review, theoretical analysis, experiment, results, conclusions and recommendations, references.

Thesis consist of: 54 p. text without appendixes, 42 figures, 4 tables, 33 bibliographical entries.

Appendixes included.

Keywords: vibrations, linear motors, modal analysis, precision positioning, frequency dynamics

Vilniaus Gedimino technikos universitetas
Mechanikos fakultetas
Mechanikos ir medžiagų inžinerijos katedra

ISBN ISSN
Egz. sk.
Data-.....-.....

Antrosios pakopos studijų **Mechanikos inžinerijos** programos magistro baigiamasis darbas 4

Pavadinimas **Precizinių pozicionavimo sistemų su tiesiniu varikliu dinaminių procesų tyrimai**
Autorius **Vilius Kavaliauskas**
Vadovas **Algirdas Maknickas**

Kalba: anglų

Anotacija

Didelė rinkos konkurencija reikalauja aukšto tikslumo bei kokybės pozicionavimo sistemų, kurios leistų gamintojams konkuruoti rinkoje. Mechaninės konstrukcijos optimizavimo jau nebeužtenka. Reikalinga dažninė sistemų analizė bei optimizavimas.

Magistro darbe atlikta precizinės pozicionavimo sistemos su tiesiniu varikliu teorinė analizė, kartu su teorine modaline analize, naudojant „SolidWorks“ programinį paketą. Surinktas eksperimentinis stendas ir atlikta praktinė dinaminė analizė bei sistemos optimizavimas.

Darbą sudaro 7 dalys: įvadas, literatūros analizė, teorinė analizė, eksperimentas, rezultatai, išvados ir rekomendacijos, literatūros sąrašas.

Darbo apimtis - 54 p. teksto be priedų, 42 iliustracijos, 4 lentelės, 33 bibliografiniai šaltiniai.

Atskirai pridėti darbo priedai.

Prasminiai žodžiai: vibracijos, linijiniai varikliai, modalinė analizė, pozicionavimo sistemos, dažninė dinamika

CONTENTS

Abbreviations	8
List of Tables.....	9
List of Figures	10
Introduction	11
1. Literature review	13
1.1. Ironless linear motor construction	13
1.2. Linear stage rigid-body construction.....	15
1.3. Controller optimization.....	18
2. Methodology	25
3. Computer simulation of precision positioning systems with linear motor	26
3.1. Creation of the model	26
3.2. Material selection	27
3.3. Mesh parameters.....	27
3.4. Analysis parameters.....	28
3.5. Analysis results.....	29
4. Experimental dynamic processes analysis of linear translation stage X axis accuracy response to velocity excitation	32
5. Results.....	37
Conclusions	51
References	52
APPENDEXES	55

Abbreviations

LSM – Linear synchronous motor

FEM - Finite element method

FTT - Fast Fourier Transform

FRF – Frequency response function

CNC - Computer numerical control

LPF – Low-pass filter

NF – Notch filter

BF – Bi-quad filter

List of Tables

Table 1 Parts and materials.....27
Table 2 Mesh parameters.....28
Table 3 Modes at different frequencies29
Table 4 Parameters of PID controllers34

List of Figures

Figure 1.1 Ironless linear motor construction [19].....	14
Figure 1.2 Thrust of different linear motor configurations [21].....	15
Figure 1.3 Example of modal shapes	16
Figure 1.4 Modal response to velocity {1,20,100,400} mm/s excitations in X configuration [26]..	17
Figure 1.5 Modal response to velocity {1,20,100,400} mm/s excitations in Y configuration [26]..	17
Figure 1.6 PID controller representations. a) Symbolistic representation; b) Time domain operator form; c) Laplace transform representation [27]	18
Figure 1.7 Proportional control [11].....	19
Figure 1.8 Example of the cascade loop system [33].....	21
Figure 1.9 Notch filter working principle	22
Figure 1.10 Low-pass filter working principle.....	23
Figure 1.11 Dynamic displacement errors of LMS platform with different controllers at different velocities and constant acceleration [12]	24
Figure 3.1 3D model of 8MTL120XY	26
Figure 3.2 Simplified 3D model of 8MTL120XY	27
Figure 3.3 Mesh of the research object	28
Figure 3.4 Mode 1 (446 Hz).....	29
Figure 3.5 Mode 2 (1 723 Hz).....	30
Figure 3.6 Mode 3 (2 254 Hz).....	30
Figure 3.7 Mode 4 (3 945 Hz).....	31
Figure 3.8 Mode 5 (5 934 Hz).....	31
Figure 4.1 FRF bode plot without filters	32
Figure 4.2 FRF bode plot PID1	33
Figure 4.3 FRF bode plot PID2	33
Figure 4.4 FRF bode plot PID3	34
Figure 4.5 Accelerometers placement scheme	35
Figure 4.6 System with 1kg load.....	35
Figure 4.7 System with 2.5kg load.....	36
Figure 5.1 System strike excitation results when 1kg load applied	37
Figure 5.2 System strike excitation produced acceleration results when 1kg load is applied	38
Figure 5.3 System results when 1kg load applied at 5mm/s velocity	39
Figure 5.4 System results when 1kg load applied at 10mm/s velocity	39
Figure 5.5 System results when 1kg load applied at 20mm/s velocity	40
Figure 5.6 System accelerations at time interval.....	41
Figure 5.7 System strike excitation results when 2.5 kg load applied	42
Figure 5.8 System results when 2.5kg load applied at 5mm/s velocity	43
Figure 5.9 System results when 2.5kg load applied at 10mm/s velocity	44
Figure 5.10 System results when 2.5kg load applied at 20mm/s velocity	44
Figure 5.11 Positioning errors at 1kg load at 5mm/s velocity.....	45
Figure 5.12 Positioning errors at 1kg load at 10mm/s velocity.....	46
Figure 5.13 Positioning errors at 1kg load at 10mm/s velocity.....	47
Figure 5.14 Positioning errors at 2.5kg load at 5mm/s velocity.....	48
Figure 5.15 Positioning errors at 2.5kg load at mm/s velocity.....	49
Figure 5.16 Positioning errors at 2.5kg load at 20mm/s velocity.....	49

Introduction

Linear synchronous motors (LSM) with ironless construction offer significant advantages for precision positioning systems, where high dynamic performance is required [1]-[2]. Linear motion is transmitted without the use of intermediate gears, screws or crank shafts, but with the use of the magnetic field [3]. Therefore, linear motors do not suffer from the problems caused by the power transmission. This kind of systems are more accurate, due to less friction and no backlash, faster, more efficient, reliable and have longer lifetime, due to mechanical construction simplicity, compared to other rotary machines [1],[2],[4].

Increased industries demand on accuracy, and wide application possibilities, ranging from medical, microscopy applications to marking, micromachining and 3D printing, makes LSM positioning systems more in demand each year [5]–[13]. Therefore, the need for research, for this kind of systems, is high to further improve the technology. Various methods have been invented to deal with the unreliability of LSM, for example disturbance observer [14], iterative learning control [15], repetitive model predictive control [16], different sliding mode control [17], and significant amount of research on the dynamic processes were done. But most of the research is based on rigid-body dynamics of the system. The lack of research on the high-frequency dynamics have become the main limiting factor for improving linear motor driven positioning systems performance and control capabilities [18].

Therefore, in this master thesis, theoretical and experimental research of dynamic processes of the precision positioning system with linear synchronous motor based on frequency domain will take place. The results will be evaluated and conclusions with recommendations will be formulated for optimization of the translation stage.

Research object

Research object - 8MTL120XY, a direct drive planar XY linear translation stage, which uses a pair of three phase ironless linear brushless servo motors. Direct drive technology enables linear stage to achieve zero backlash motion, resulting in high accuracy, repeatability and low friction. Used for accurate positioning of photonic or other instruments.

Main problem

The aim of the master thesis is to analyze dynamic processes that have effect on precision positioning systems with linear synchronous motors accuracy, when the system is excited by different velocities.

Newness of the topic

Not many research papers are written about frequency dynamics of high precision translation stages with linear motors, and negative effects of dynamic processes persist. Also, no known research was performed on the investigated research object. Therefore, this system is chosen for the master thesis research.

Relevance of the topic

The optimization of the linear translation stage reduces negative effects of the dynamic processes and allows to increase positioning accuracy. This leads to greater results in experiments, which involve linear translation stages, and other applications. In the master's thesis, recommendations and conclusion will be presented of how to modify the system.

Goal of research

Goal of the research is to analyze dynamic processes effects on X axis of 8MTL120XY translation stage with linear motors accuracy.

To achieve research goal, these steps must take place:

1. Analysis of scientific literature, which research linear motor construction.
2. Analysis of scientific literature, which research controller parameters effects on precision positioning systems with linear motors.
3. Perform modal analysis of the 8MTL120XY linear stage.
4. Perform experimental research of translation stage with linear motors to determine effect of dynamic processes to the stage accuracy.
5. Formulate conclusions and recommendations.

Research results will be evaluated using „Microsoft Office Excel“, “Origin Pro 9.0”, „SolidWorks Simulation“, “PULSE LabShop”, “ACS SPiiPlusSC” software packages.

1. Literature review

Precision positioning systems with linear ironless motors are widely used in the industry, due to their advantages over rotary machines, and high accuracy. The three components that contribute to positioning systems with linear ironless motors positioning accuracy are analyzed in this master thesis:

- Motor construction
- Linear stage rigid-body construction
- Controller optimization

1.1. Ironless linear motor construction

Ironless linear motors are used in 8MTL120XY linear translation stage. They provide low weight forces, wide air gap (for easy installation and alignment), fast acceleration, and eliminates cogging, which results to super smooth motion [19].

Ironless linear motors construction consists of primary part and secondary part. Primary part is coil assembly, which is made by placing overlapping coils in precisely molded resin epoxy shell and vacuum molding entire assembly to eliminate air bubbles. This kind of assembly process provides the coil assembly high force density, enhanced lifetime, high heat dissipation, and great dielectric strength, which results to high system stability. Secondary part is magnetic way. This part of ironless linear motor consists of two parallel steel plates, which are joined at one end to created gap for the primary part to move. Steel plates have embedded rare-earth magnets, which are embedded in alternating way and different polarities magnets are facing each other. This kind of configuration of magnets are known as Halbach array or U channel[20]. Two magnetic ways gives ironless linear motor more effective utilization of the induced flux from both sides.

Due to ironless linear motor unique construction, depending on which part is fixed, coil assembly can move along magnetic way, or can force magnetic way to move, and act as forcer. In 8MTL120XY direct drive planar XY linear translation stage, coil assemblies are fixed, and magnetic way moves linearly.

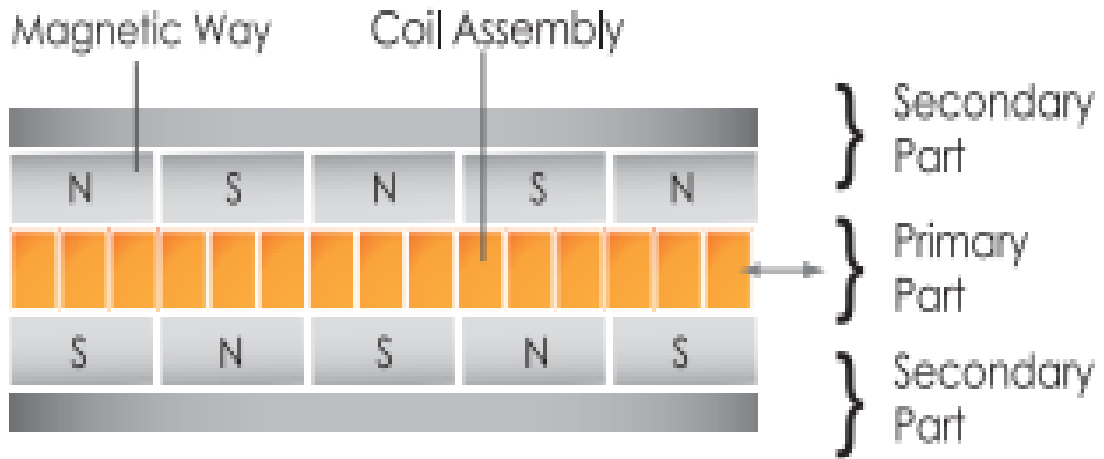


Figure 1.1 Ironless linear motor construction [19]

Linear machines working principle is the same as rotary counterpart: magnetic flux from mover (rotor) is locked or synchronized with that of a stationary track (stator) converting electromagnetic energy into translation motion [2]. In other words, applied three-phase current to three adjoining coils of the translator leads to a sequence of attracting and repelling forces between the poles and the permanent magnets. This results in a thrust force, which in linear motors is generated by “Lorentz force” induced proportionally to the added current:

$$\vec{F} = I\vec{L}\vec{B} \quad (1.1)$$

Where:

B – strength of the magnetic field

L – length of the wire

I – current

F – magnetic force

Also, the linear synchronous motors are operating on the principle of traveling magnetic field, the speed of the moving part v is the same as the synchronous speed v_s of the travelling magnetic field, which depends on frequency and pole pitch, but does not depend on the number of poles [3]:

$$v = v_s = 2f\tau = \frac{\omega}{\pi}\tau \quad (1.2)$$

Where:

v – speed of the moving part

v_s – synchronous speed of the travelling magnetic field

f – input frequency

τ – pole pitch

ω – angular input frequency

Force fluctuations in linear motors systems cause negative effects to the accuracy. Ironless linear motors with Halbach array have an advantages on this issue due to having highest average thrust force compared to axial and radial configurations as shown in Figure 1.2 [21]. This allows to achieve smoother linear movement, and due to lower forcer mass allows to achieve high acceleration rates [2].

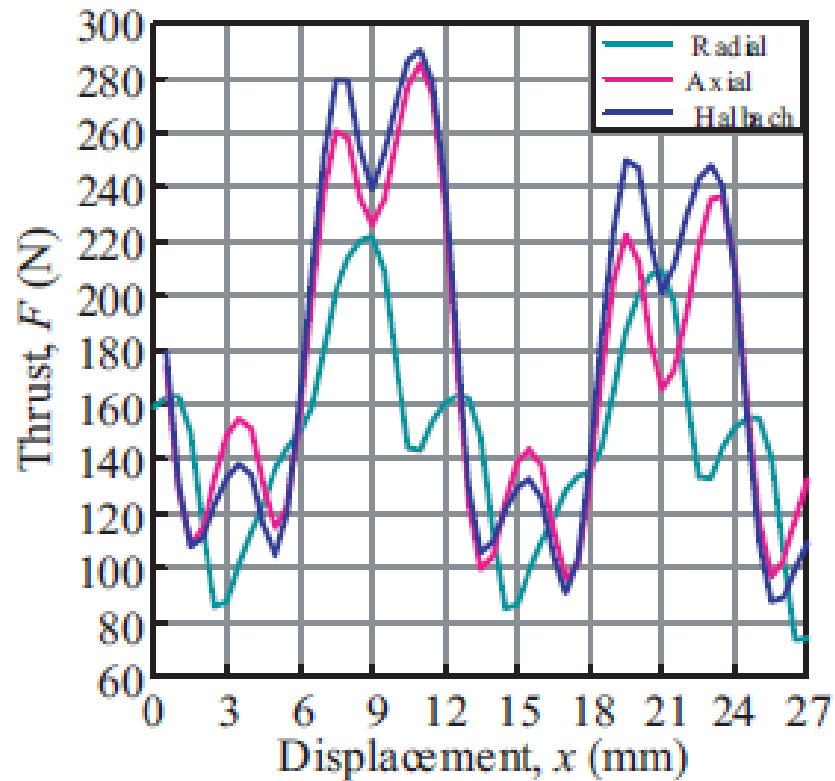


Figure 1.2 Thrust of different linear motor configurations [21]

1.2. Linear stage rigid-body construction

Rigid-body analysis of any construction allows to determine the weak points of the construction, and the natural frequencies of the system that should be avoided to reduce the damage on the system after periodic loading. The analysis is done using finite element method (FEM) or experimentally.

Modal analysis focusses on the dynamic properties of systems in the frequency domain. It is a useful tool, which provides a definitive description of the response of the structure. With the information gathered from modal analysis, it is possible to determine the eigenfrequencies (f), damping ratios (ζ), and modal shapes (ϕ) of the system. This allows to ensure the avoidance of resonance frequencies, which can damage the system after periodic loading.

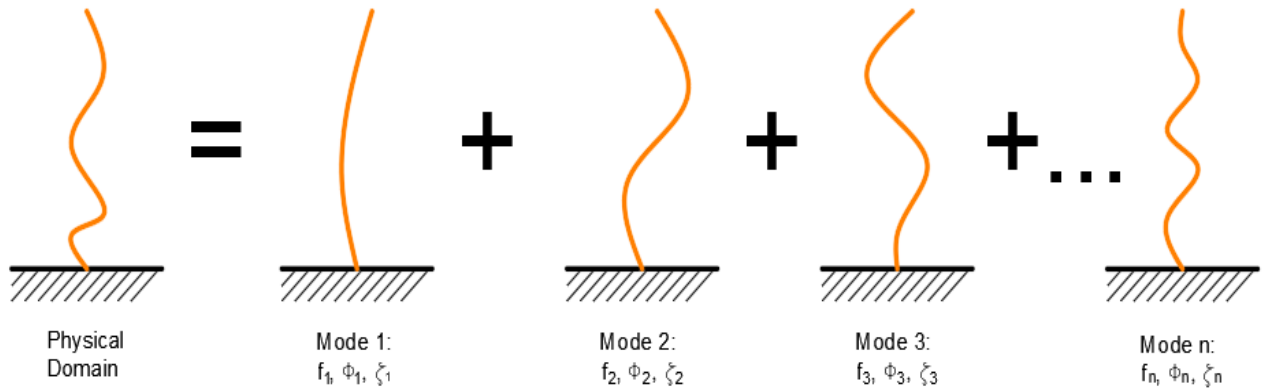


Figure 1.3 Example of modal shapes

To perform modal analysis experimentally, the system must be excited by an external force and measurements of input force and output acceleration must be taken. Using Fast Fourier Transform (FTT), obtained signals are transferred to frequency domain. This creates unput force spectrum and output acceleration spectrum, which are both separated to obtain frequency response function (FRF)[22]. FRF is a function used to quantify the response of a system to an excitation, normalized by the magnitude of this excitation, in the frequency domain [23].

In the research written on the bus frame optimization using alternative materials, strength and stiffness of the frame was taken as key indicators of the structure performance. Stiffness is particularly important parameter of the rigid construction. The lack of stiffness introduces noise and vibrations, which negatively effects the accuracy of the system in precision positioning systems, but in this case, it negatively effects the comfort of the passengers. By performing modal analysis of the bus frame, the authors optimized the structure and improved its dynamic performance by 20% and reduced mass of the frame by 11%, by replacing some materials of the structure from steel to fiberglass, without sacrificing the safety characteristics of the vehicle [24].

In another study done on computer numerical control (CNC) lathes driven by linear motor, FEM modal analysis were performed on slide board to determine the maximum deformations and their position. It was determined that the maximum deformations occurred where the linear motor was placed on slide board. Based on simulation results, linear motor feed system control parameters were selected. Also, the research results showed that the position loop proportional gain, speed loop proportional gain and speed loop integral response time are the biggest influence factors on servo dynamic stiffness. The displacement response is reduced under the cutting interference force step inputting, while the position loop proportional gain, speed loop proportional gain and speed loop integral response time are increased, and the servo dynamic stiffness is increased, the number of system oscillation is also reduced, and the system tends to be stable [25].

The last analyzed research paper written on the linear stage with quasi-industrial guiding system modal and dynamic response to velocity excitation, showed the importance of modal analysis of positioning system with linear motors for FRF adjustment. The modal analysis was done to determine the natural frequencies of the research system. Based on the results, the suggestions were made of how to reduce the significance of natural frequencies on the system accuracy, by adjusting controller parameters, like bandwidth. Also, the results showed, that X configuration system is significantly influenced by lower bandwidth frequency excitation, while Y configuration spectral response bandwidth is wider [26].

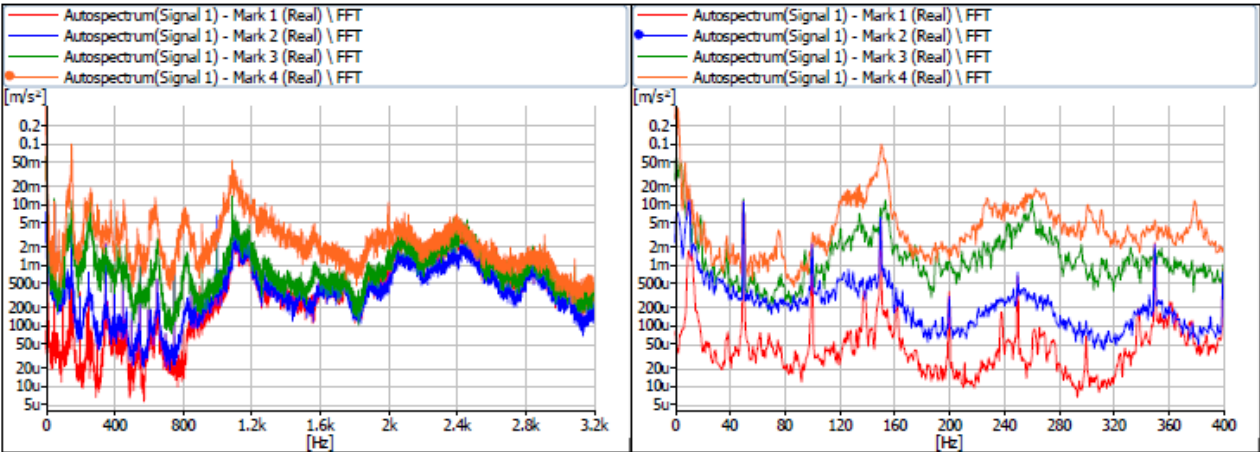


Figure 1.4 Modal response to velocity {1,20,100,400} mm/s excitations in X configuration [26]

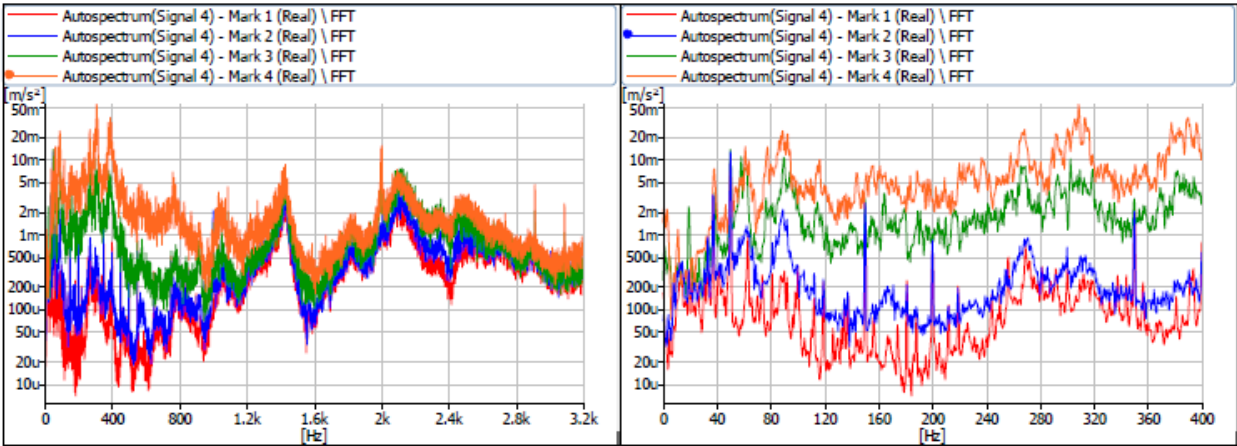


Figure 1.5 Modal response to velocity {1,20,100,400} mm/s excitations in Y configuration [26]

1.3. Controller optimization

Well optimized controller for the specified task of the system can unlock the full potential of the designed system. There are many types of the controller design architectures, but the most common one is PID controller.

PID controller

“Proportional, integral and derivative controller (PID controller)” is a control loop mechanism and the most common form of feedback. The ease of use and the provided efficient solutions to the most real-world control problems, made PID controller the standard tool for process control. Around 90-95% of all the controls loops are of PID type, just more advanced versions [27],[28],[29],[30]. The PID is an equation that the controller uses to evaluate the controlled variables. A process variable is measured, and the feedback signal is then sent to the controller, which compares the feedback signal value to the set point value and establishes the error value. After establishing the error value, the controller issues the necessary commands or adjust the control variable to correct the error. The process is performed iteratively to maintain desired parameters of the system with the lowest error possible. The PID controller can run in manual or automatic mode. In manual mode, the controller output is manipulated by the operator, and during automatic mode – the parameters can be altered during PID controller operation [31].

The general equation for the PID algorithm is described as:

$$u(t) = K \left(e(t) + \frac{1}{T_i} \int_0^t e(\tau) d\tau + T_d \frac{de(t)}{dt} \right) \quad (1.3)$$

But it can be further simplified to three components:

$$\text{control variable} = P_{out} + I_{out} + D_{out} \quad (1.4)$$

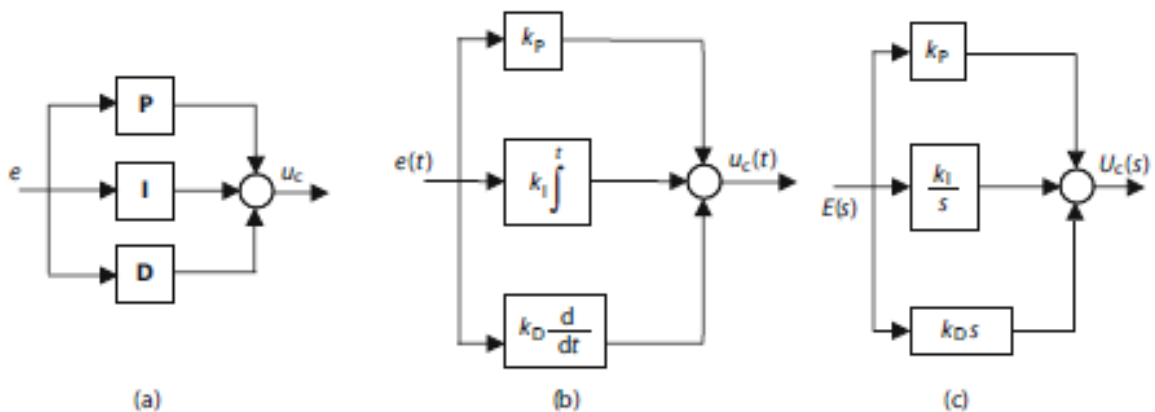


Figure 1.6 PID controller representations. a) Symbolic representation; b) Time domain operator form; c) Laplace transform representation [27]

Proportional control

The proportional element of PID controller regulates the reaction proportionally based on the current error. Mathematically it is expressed as:

$$P_{out} = K_p e \quad (1.5)$$

Where:

P_{out} – proportional portion of the controller output

K_p – proportional gain

e – error signal

Proportional control systems only respond to the magnitude of the error and not to its rate of change. Therefore, proportional control cannot compensate for the very small errors in the system. The Figure 1.7 shows proportional control. From the figure it is seen that the proportional control system always has a steady state error, which decreases with the increase of proportional gain. It must be noted, that increase in gain leads to larger output or faster response of the system to the given input error, and smaller gain results in the less responsive control. But too large proportional gain results in process instability and oscillation as it can be seen in the figure.

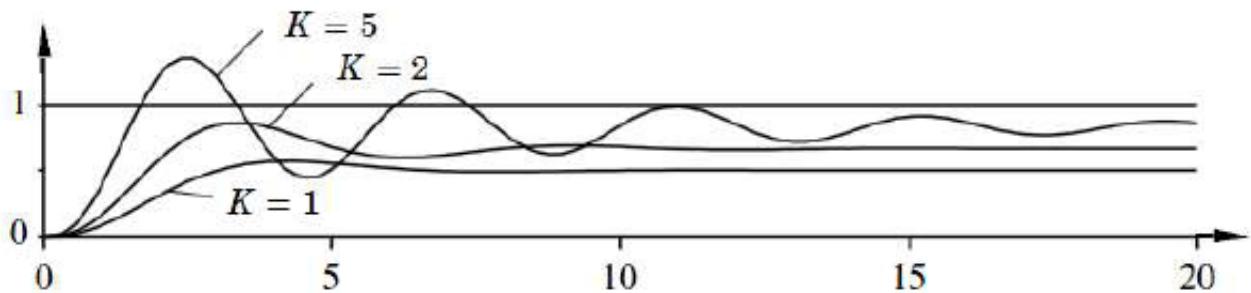


Figure 1.7 Proportional control [11]

Integral control

The integral control tries to correct the small error. It examines the error over time and increases its importance over time, by multiplying the persisted error by the time it has persisted. By doing this, the integral control increases the system response to the given error until the system controller corrects the given error. Also, the integral can be altered, which is called the reset time. It must be noted, that the shorter reset time leads to the quicker correction of the given error, but can cause erratic performance of the controlled system. The mathematical expression of the integral control is:

$$I_{out} = \frac{1}{T_i} \int e dt = K_i \int e dt \quad (1.6)$$

Where:

I_{out} – integral portion of the controller output

T_i – integral time, or the reset time

K_i – integral gain

e – error signal

Derivative control

Derivative control element of the PID controller tries to focus on the rate of change in the error signal. The greater rate of change leads to greater system response. The derivative is altered as a time factor, and because of this is called rate time. Too much of derivative results in overshoot and erratic control of the system. Mathematically derivative is expressed as:

$$D_{out} = T_d \frac{d}{dt} e = K_d \frac{d}{dt} e \quad (1.7)$$

Where:

D_{out} – derivative portion of the controller output

T_d – derivative time

K_d – derivative gain

e – error signal

Velocity, position, and current loops

Control loop is a process of monitoring feedback and making corrections [32]. It consists of physical components control function, which adjust measured variables to the specified requirements. Depending on the requirements, system can have a combination of three types of control loops: current loop, position loop or velocity loop.

Velocity loop compares set velocity value with the measured velocity value via tachometer or encoder and adjusts the motor speed to achieve specified velocity. This type of loop commonly uses both proportional gain and integral gain to regulate correction commands. Proportional gain is directly proportional to error size, and integral gain builds up over time to correct the motor at the end of the action.

Position loop determines deviation between actual position and set value. After evaluating the deviation position loop corrects velocity to reduce or eliminate occurred position error. Therefore, position loop is added to velocity loop, and velocity loop must be tuned first. Position loop typically uses proportional gain only.

Current loop is used to control torque, which affects velocity and position. Current loop parameters are usually adjusted by the manufacturer, in order to save time and struggle for the user.

All mentioned loops can be used in cascade system (Figure 1.8), where outer loop generates commands to the inner loop. But for the inner loop to take effect on the outer loop its response time must be faster than the outer loop. To make the loop faster it must have higher bandwidth and work at higher frequency zone. Higher bandwidths leads to the better overall stability, but can cause reduction of the performance of the system, when unachievable response times are reached [32],[33].

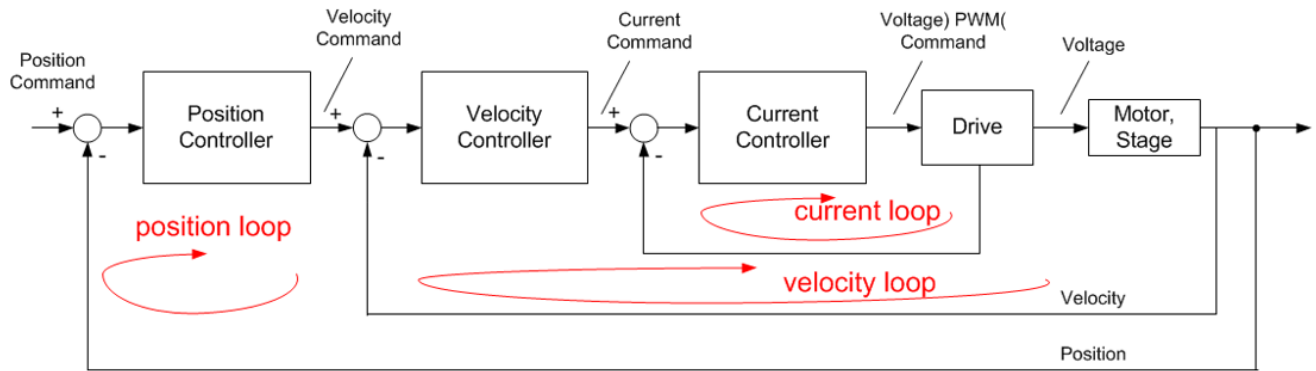


Figure 1.8 Example of the cascade loop system [33]

Filters

To achieve better signal quality and to eliminate unwanted characteristics of the signal, before it is used in calculations or in a controller, filters are used. Filters modify the calculated, or measured signal by the sensors by using logic and/or algorithms. Filtering process reduce and smoothen out high-frequency noise, but can introduce lag in the control and cause instability, when it is overdone. There are a lot of different filters used for specific needs of modifying the signal to achieve desired results.

1. Notch filter

Notch filter (also known as band stop or reject filter) is used to remove a narrow band of frequencies. In other words, notch filters allow to pass the frequencies below or above the notch frequency. This type of filter causes little phase lag in the control loop and can remove the resonance from the system. Notch filters disadvantage is that it can only work on narrow band of frequencies and have to be tuned for the frequency of resonance or of noise generation. Common structure of the notch filter transfer function:

$$F_r = \frac{s^2 + 2\zeta\omega s + \omega^2}{(s + \omega)^2}, \zeta \ll 1 \quad (1.8)$$

Where,

ω – the resonance frequency of the system

ζ – damping ratio

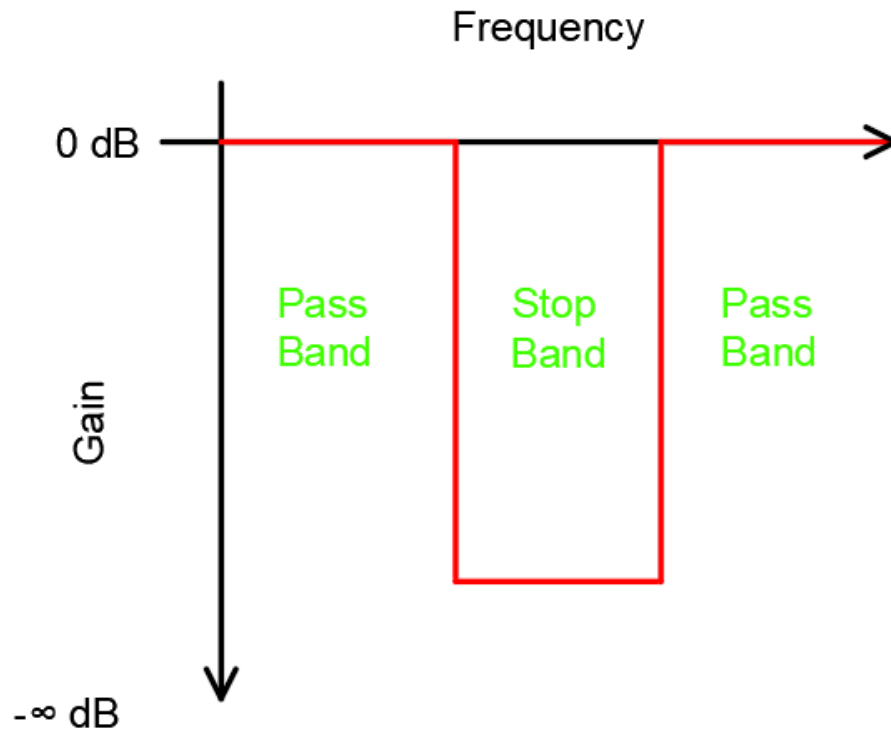


Figure 1.9 Notch filter working principle

2. Kalman filter

Kalman filters are algorithms, that optimally estimates unknown variables of interests, when only indirect measurements are available, by observing information over time. Also, this type of filters are used to obtain the closest estimates of state, using information gathered from various sensors in the presence of noise. Kalman filters have lower computational power requirements due to their relatively simpler form, but require the user to be familiar with estimation theory to be successfully implemented.

3. Low-pass and high-pass filters

Low-pass filers are used for passing the signals, which have frequencies lower than the selected frequency in the filter, and to reduce frequencies that are higher than selected frequency. Mathematical expression:

$$H(s) = K \cdot \frac{\omega}{s + \omega} = K \cdot \frac{\omega^2}{s^2 + 2\beta\omega s + \omega^2} \quad (1.9)$$

Where,
 K – gain
 β – damping

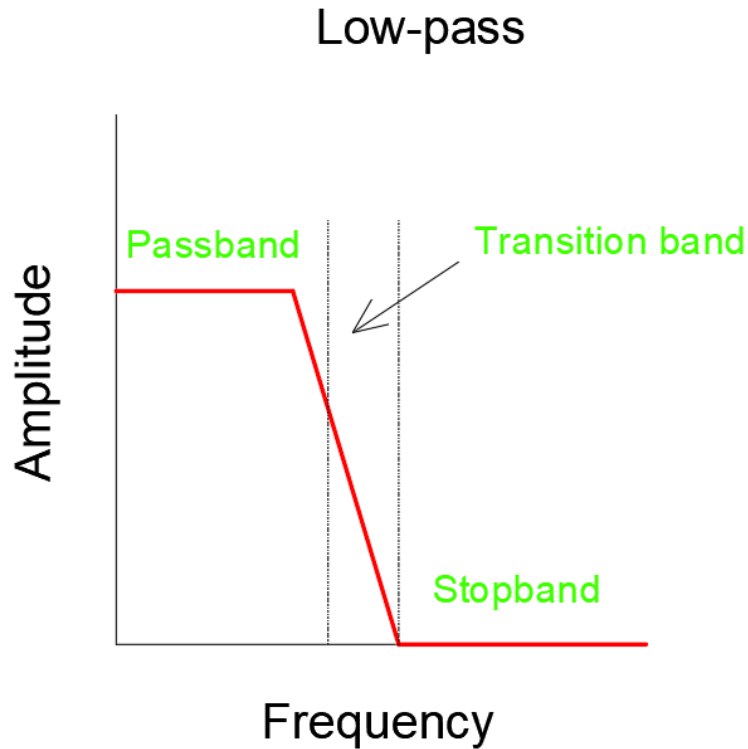


Figure 1.10 Low-pass filter working principle

High-pass filters are a complement to the low pass filters. They operate oppositely to low-pass filters, by passing signals with higher frequencies than selected frequency in the filter. Mathematical expression:

$$H(s) = K \cdot \frac{s}{s + \omega} = K \cdot \frac{s^2}{s^2 + 2\beta\omega s + \omega^2} \quad (1.10)$$

Low-pass and high-pass filters help to reduce or completely eliminate noise and get a clean desired signal, without unwanted frequencies.

4. Bi-quad filter

It is a general 2nd order filter with quadratic terms, one in the numerator, and another one in the denominator. Can be thought as a high-pass filter in series with a low-pass filter. Several cascaded filters can help to shape the frequency response by compensating or attenuating mechanical resonance, improving phase and gain margins, and increasing the bandwidth. Mathematically expressed:

$$H(s) = \frac{\left(\frac{s}{\omega_N}\right)^2 + 2\zeta_N\left(\frac{s}{\omega_N}\right) + 1}{\left(\frac{s}{\omega_D}\right)^2 + 2\zeta_D\left(\frac{s}{\omega_D}\right) + 1} \quad (1.11)$$

In analyzed research paper, which investigated the dynamic errors of the displacement of the platform of the one degree of freedom long-travel linear motor stage with air bearings by applying different controllers consisting of a low-pass (LPF), notch (NF), and second-order bi-quad (BF) filters at different velocities. The plant was excited by the frequency based sinusoidal current of the constant amplitude, while the system was moving at constant speed. The accelerometer was used to compare identified eigenfrequencies to the harmonic excitation obtained by the frequency response function (FRF) of the plant investigated. The configurations on the controllers were: PID1 (where only LPF is used), PID2 (where LPF and NF are used) and PID3 (where LPF, NF and BF are used). It was determined that higher-order controllers can reduce the dynamic error significantly at low velocities of the moving platforms: 1 and 5 mm/s. But also, the low order controllers of 4th-degree polynomials of the transfer function can also provide small dynamic errors of the displacement of the platform [12].

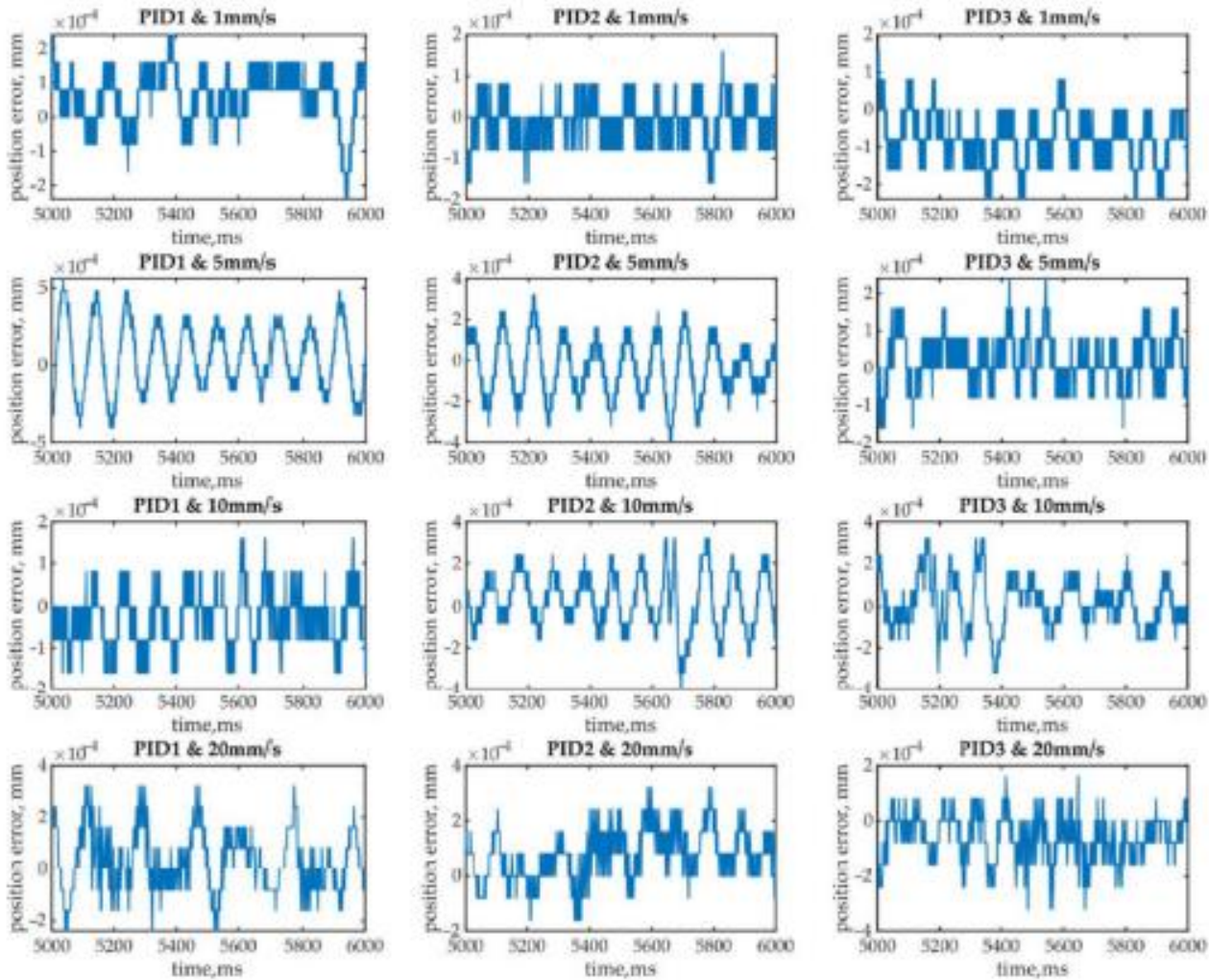


Figure 1.11 Dynamic displacement errors of LMS platform with different controllers at different velocities and constant acceleration [12]

2. Methodology

Used equipment

“Standa 8MTL120XY” - direct drive planar XY linear translation stage

“Standa 1TS” - optical table

“Standa 1HB” – honeycomb optical breadboard

“ACS UDMlc” - universal drive module

“Brüel & Kjær” – accelerometers system

Accelerometers

Methodology

Based on research analyzed in rigid-body construction [24], [26], the modal analysis of the research object must be made.

Theoretical research is performed by creating the 3d model of the research object and simplifying it using “SolidWorks 2020”. The model simplification is performed to reduce the chance of simulation errors and to speed up the simulation, without sacrificing simulation accuracy. Gathered results from modal analysis will show the natural frequencies of the positioning system, which should be avoided or damped using PID controllers to reduce the chance of damage to the system.

After the modal analysis of the research object, the experiment setup must be done. The research object is placed on the optical table to ensure stability. Accelerometers then are placed on the optical table and on the research object to collect data for the FRF analysis. Research object is then connected to the controller, and accelerometers are connected to the accelerometers system, which are then both connected to the PC. Using controller FRF analyzer the position and velocity loops are optimized for the best performance based on research [25].

Using FRF analysis PID controllers with different architectures are then optimized using controller software FRF analyzer. The linear stage is then programmed to move at different velocities based on the research analyzed in controller optimization chapter [12]. When the linear stage is moving at constant speed the data from the accelerometers and linear stage control software are saved and analyzed.

The experiment is then repeated with added different loads. Load is applied on the top of the linear stage at the center.

3. Computer simulation of precision positioning systems with linear motor

The aim of this simulation is to find the eigenfrequencies of the research object, 8MTL120XY linear stage. Eigenfrequencies will show the frequencies, which should be avoided. At specified frequencies the system can achieve resonance, which can damage the system after periodic loading.

3.1. Creation of the model

The model of the research object is created using “SolidWorks 2020” software package. All measurements are taken from real object, and each part is design to be as close to real life object as possible. Entities that do not have a lot of impact on the frequency domain analysis are deleted to reduce the complexity of the object and to avoid meshing errors. The frequency analysis is done using “SolidWorks 2020” add-in “SolidWorks Simulation”.

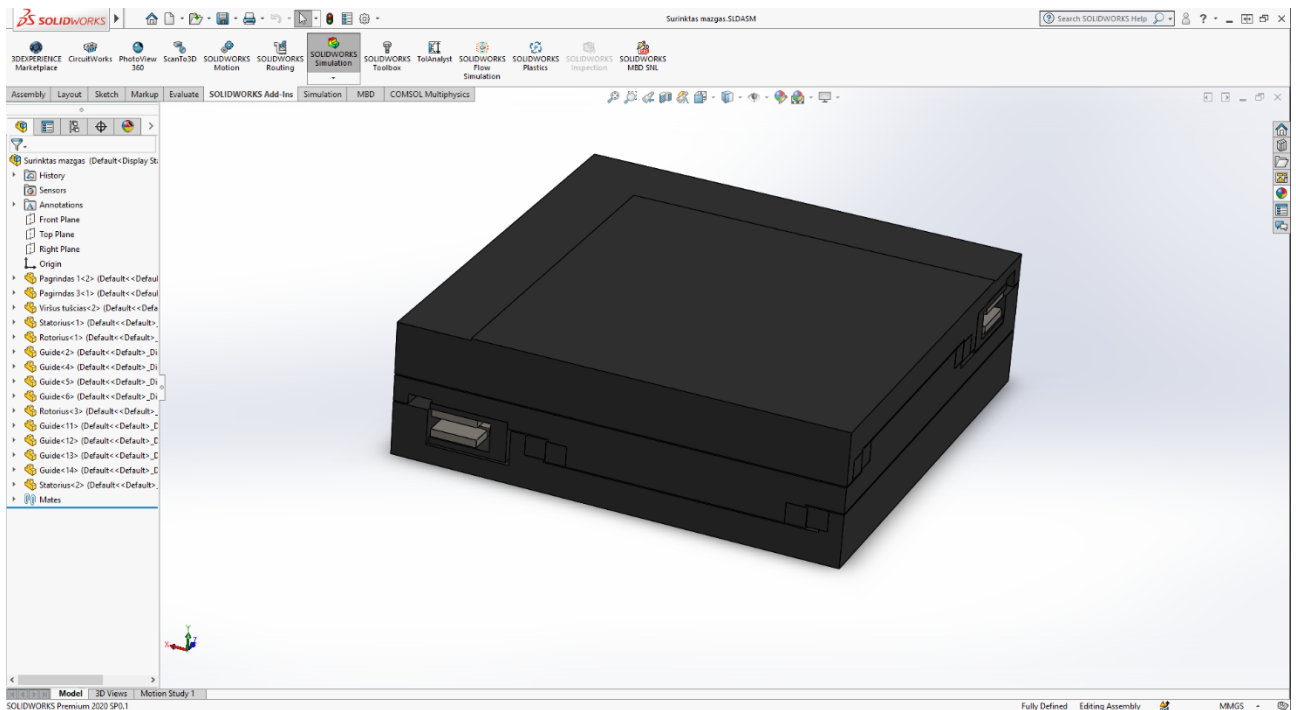


Figure 3.1 3D model of 8MTL120XY

Figure 3.1 shows the 3D model of the 8MTL120XY linear stage. The model is further simplified, by merging the Y axis with the middle plate. It is done to imitate the combination of plates by connection plate used during the experiment, because only X axis is used in the experiment. Also, all threads and other screw holes, unimportant edges, Y axis linear motor are removed. The simplified model is shown in Figure 2.2.

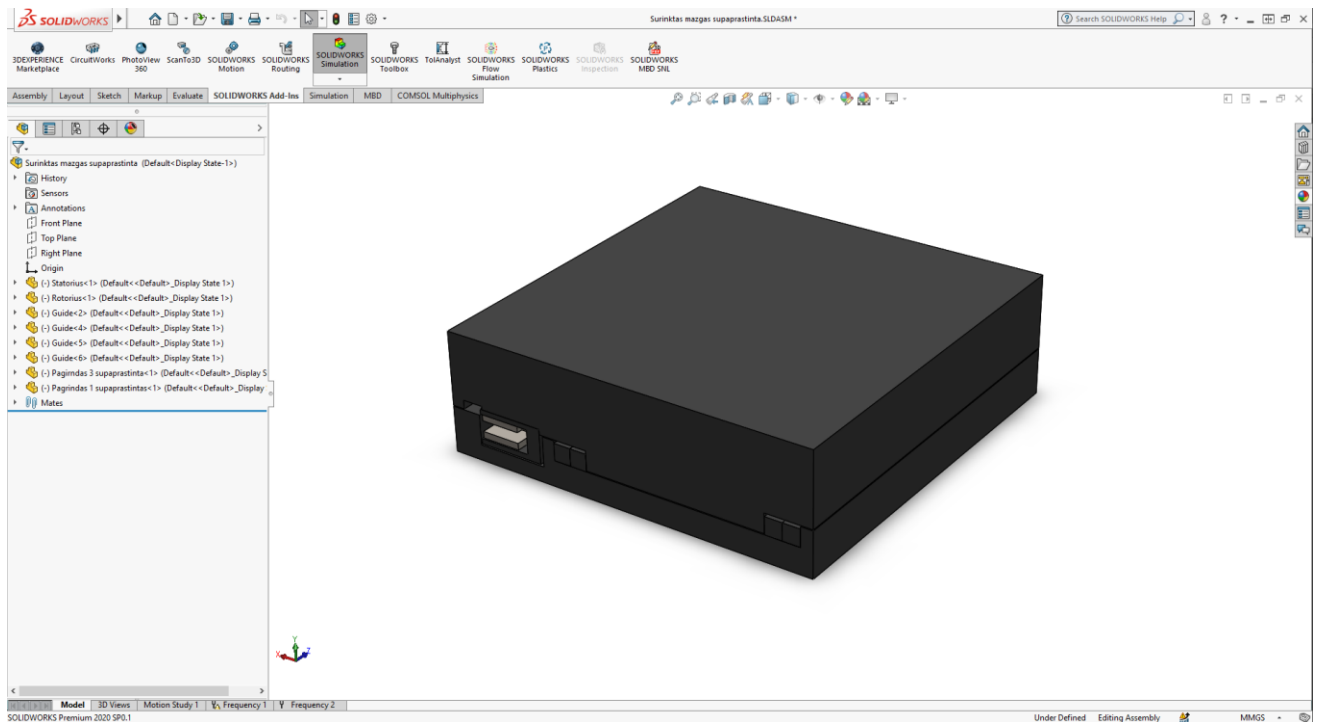


Figure 3.2 Simplified 3D model of 8MTL120XY

3.2. Material selection

Materials were selected to be the same as real life objects materials. All materials of the parts are listed in Table 1:

Table 1 Parts and materials

Part name	Selected material
Guide	Steel
Rotor of the motor	Steel
Forcer of the motor	Epoxy resin
Bottom plate	7021 aluminum
Top plate	7021 aluminum

3.3. Mesh parameters

“SolidWorks Simulation” uses finite element method (FEM) to solve the approximate solutions to differential equations. FEM divides model into finite elements, which is called mesh. Size of the mesh is selected to be “Fine”, quality “High”. Element shape is selected as “Tetrahedron”. A tetrahedron has 4 vertices, 6 edges, and is bounded by 4 triangular faces.

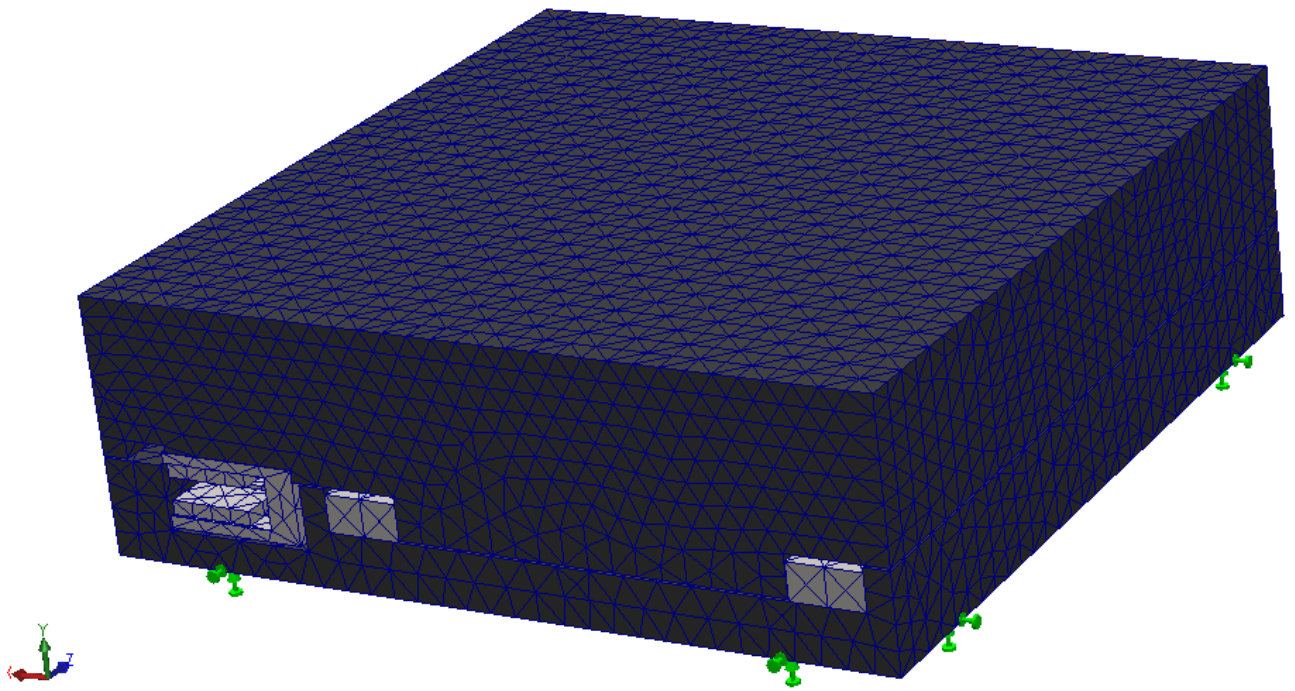


Figure 3.3 Mesh of the research object

Table 2 Mesh parameters

Description	Value
Biggest element size (mm)	8
Smallest element size (mm)	1.6
Number of elements	79869
Number of nodes	125800

3.4. Analysis parameters

Before computing the frequency domain analysis initial conditions are set. In “SolidWorks Simulation” add-in “Frequency study” is selected. Bottom surface of the research object is fixed, and in external loads gravity is applied. After setting initial conditions, “Run this study” button is pressed and then it is waited for the software package to finish the needed calculations to solve the natural frequencies problem.

3.5. Analysis results

Using analysis and “SolidWorks Simulation” software package the visual results of 5 modes that have effects on X axis at different frequencies are obtained:

Table 3 Modes at different frequencies

Mode name	Frequencies (Hz)
Mode 1	446
Mode 2	1 723
Mode 3	2 254
Mode 4	3 945
Mode 5	5 934

All mode shapes are visualized in Figures 3.4 – 3.8. The amplitudes of X (AMPX), Y (AMPY), and Z (AMPZ) axis are summed and represented by resulted amplitude (AMPRES). The visualizations are not to actual scale. They are hyperbolized for better understanding of how the linear stage deforms.

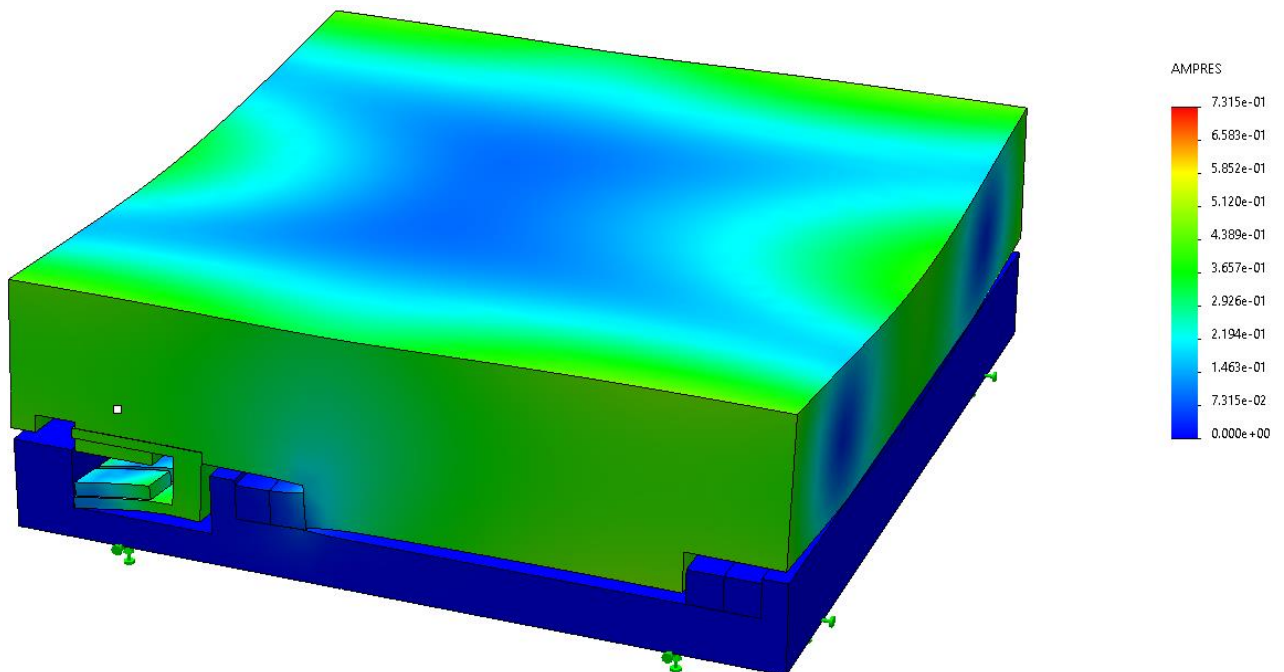


Figure 3.4 Mode 1 (446 Hz)

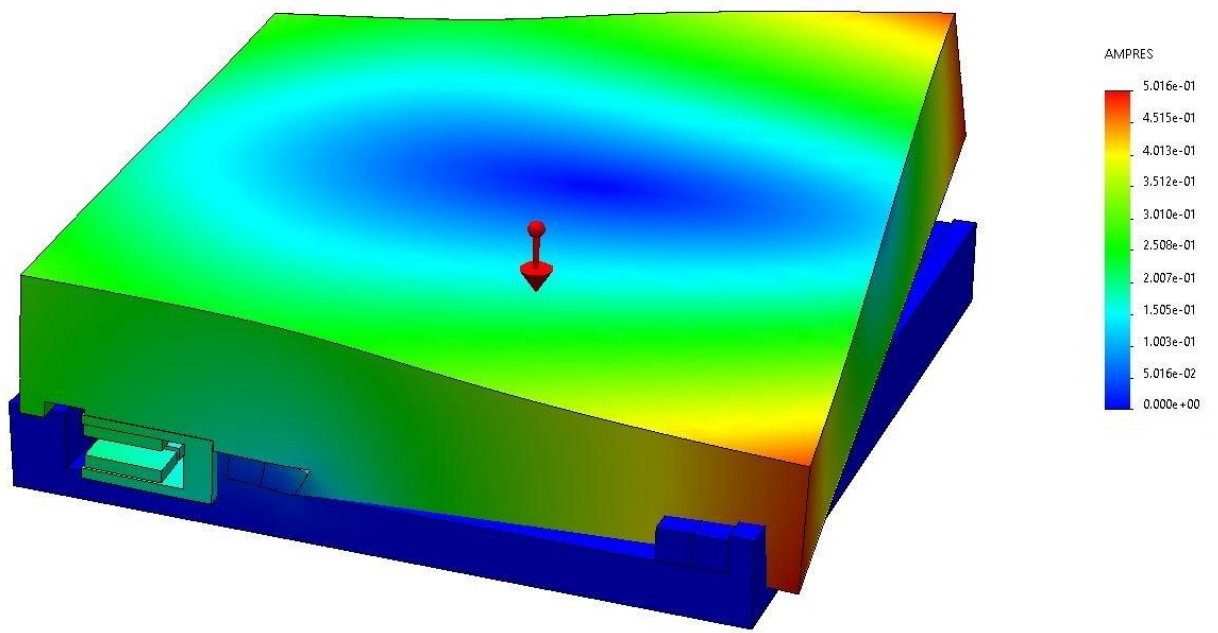


Figure 3.5 Mode 2 (1 723 Hz)

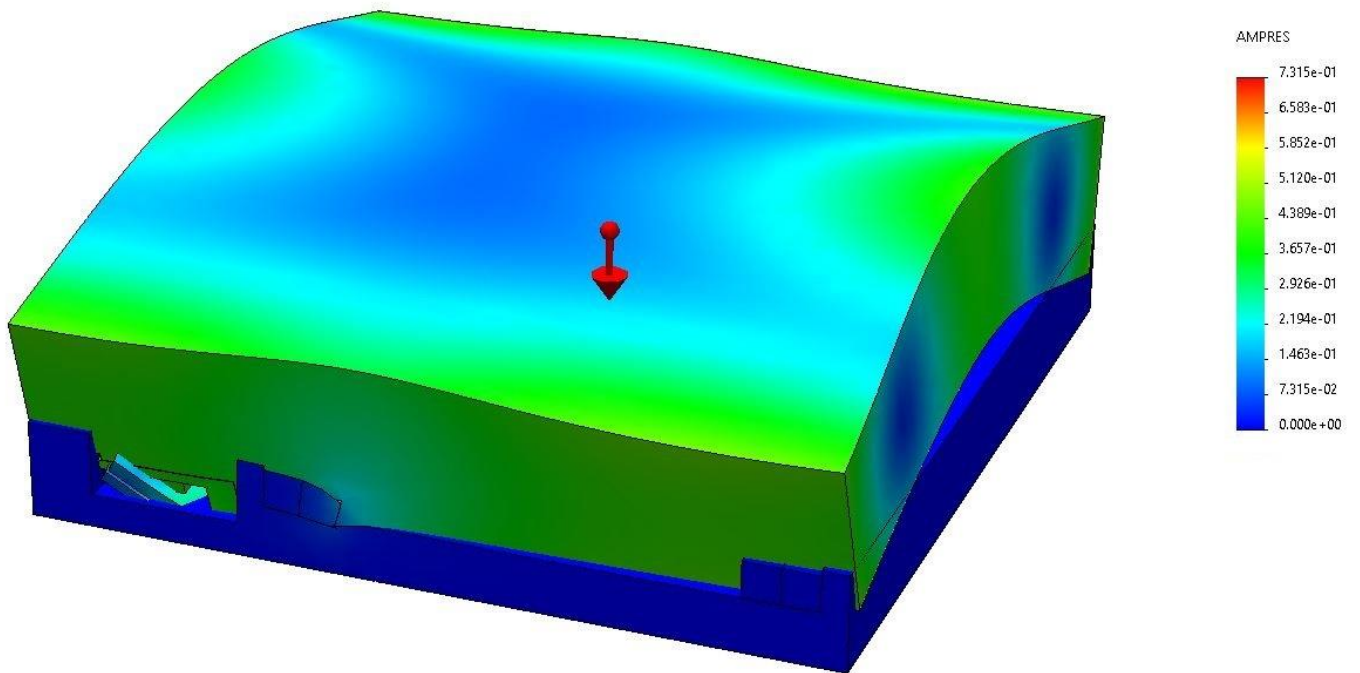


Figure 3.6 Mode 3 (2 254 Hz)

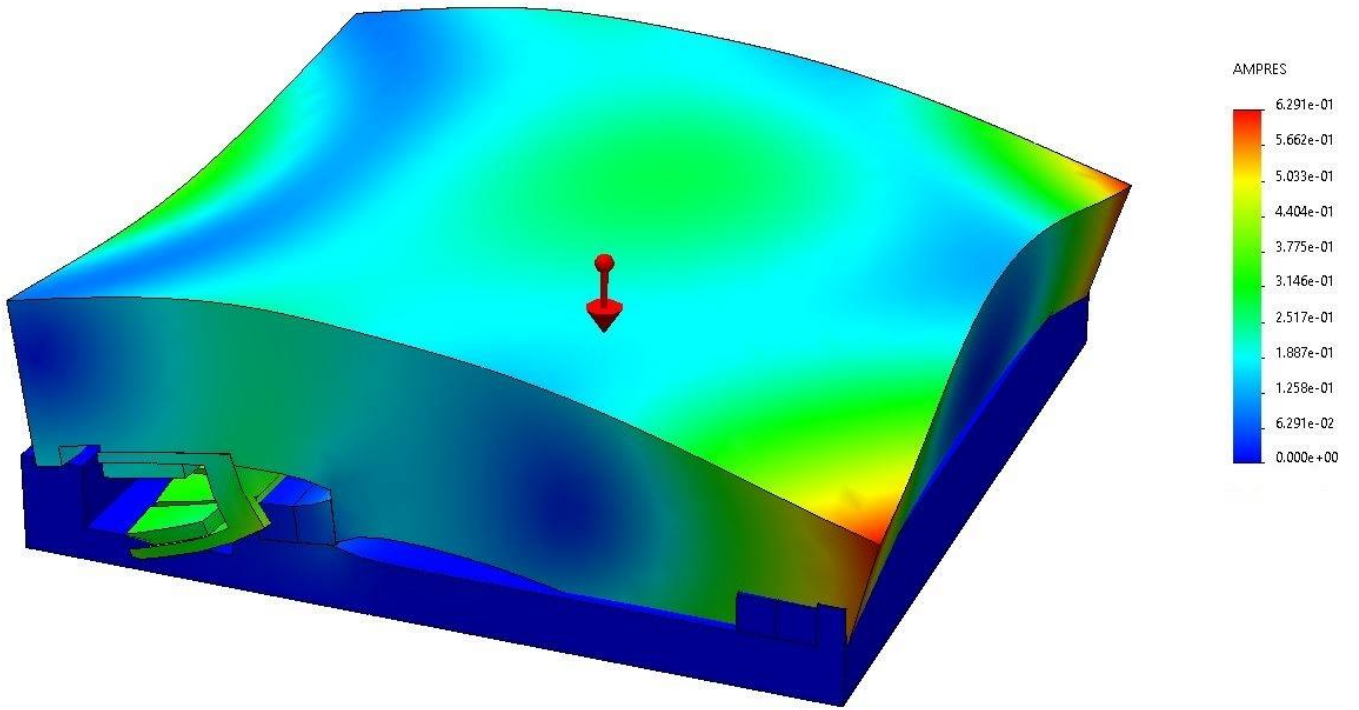


Figure 3.7 Mode 4 (3 945 Hz)

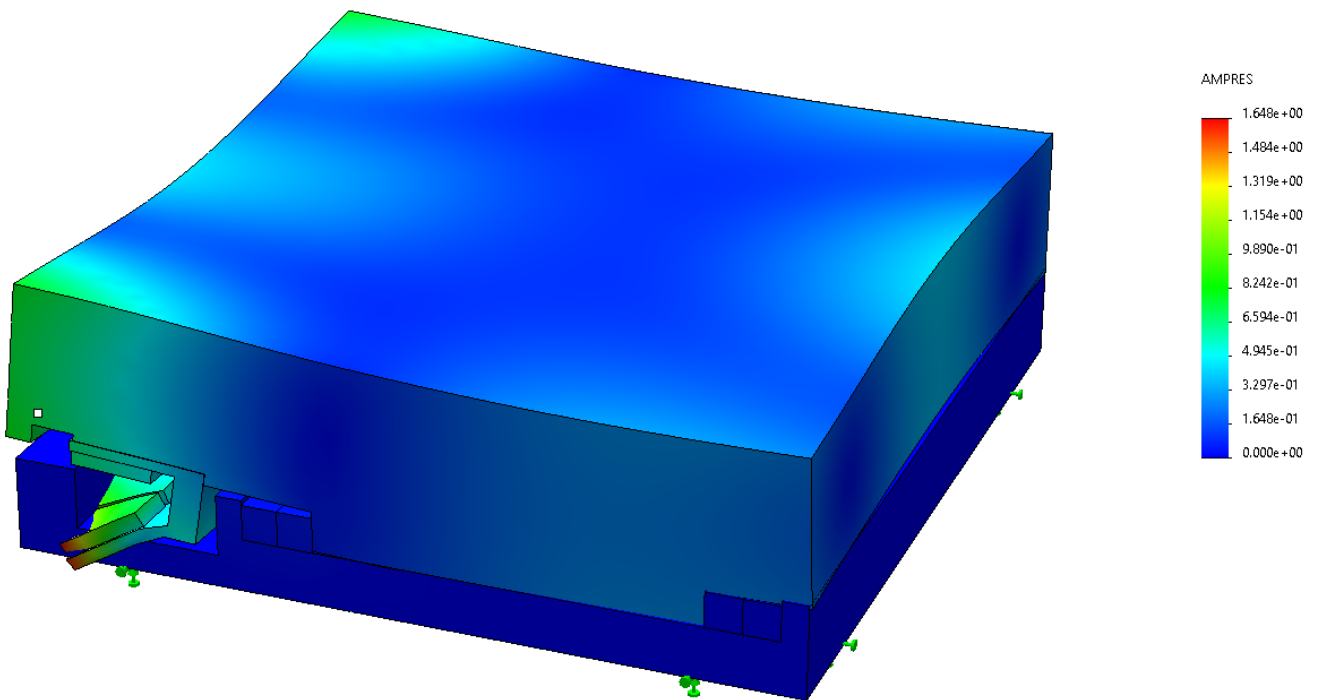


Figure 3.8 Mode 5 (5 934 Hz)

4. Experimental dynamic processes analysis of linear translation stage X axis accuracy response to velocity excitation

The experiments were done in the Vilnius Tech faculty of mechanics, mechanical engineering experiments laboratory, with provided equipment of Vilnius Tech university.

The precision positioning system with linear motor performance can be altered using different PID controller architectures. The importance of PID controller filters are determined by the linear stage mounting area quality, applied load and applied load position from the center of mass, and velocity.

During the experiment, the frequency and dynamic characteristics measurement and analyzation equipment was used: DELL computer with “ACS SPiPlusSC” software package, used to control the linear stage parameters, and “Brüel & Kjør” accelerometers system, used to collect data and analyze it using “PULSE LabShop” software package.

Linear translation stage was placed on optical table for better stability. Y axis of the research object was locked using transportation plate, and only X axis was used in the experiment. Velocity and position loops optimization was performed using “ACS FRF analyzer”, which allows to simulate effects of the selected parameters, without the need to re-measure. Optimized FRF bode plot is shown in Figure 4.1.

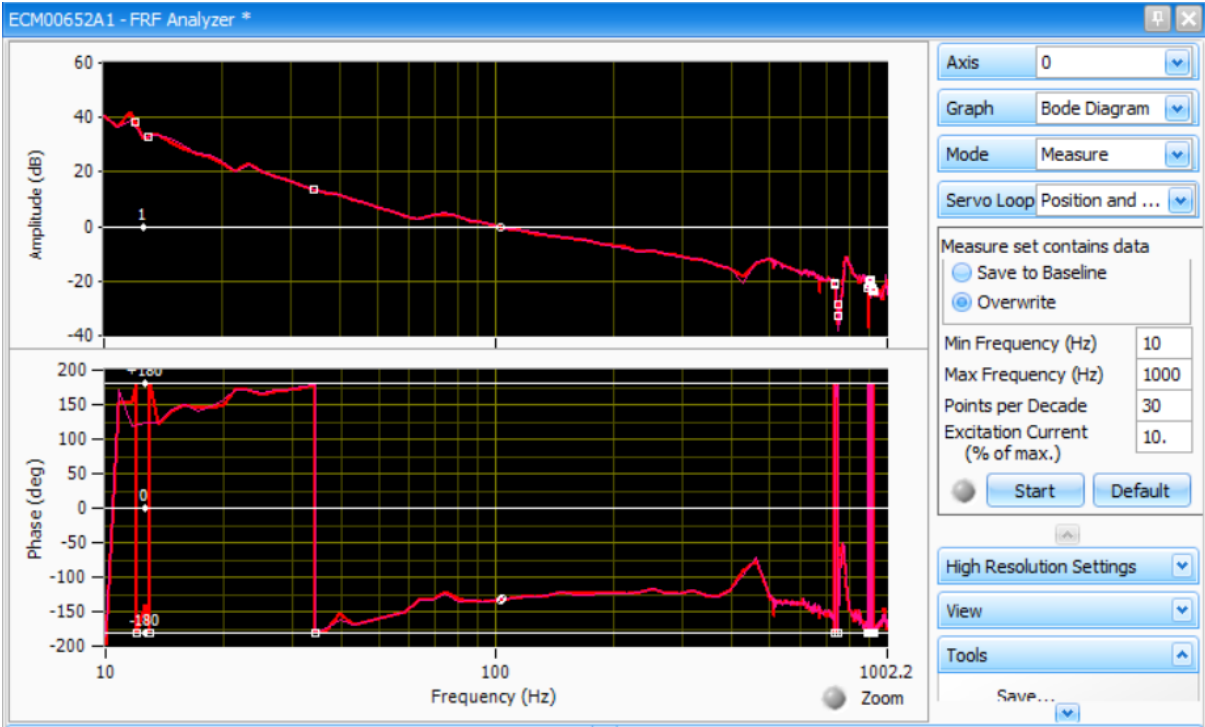


Figure 4.1 FRF bode plot without filters

After velocity and position loops optimization, three PID controller filters configurations were applied to the linear stage controller: PID1 (low pass filter), PID2 (low-pass and notch filters), and PID3 (low-pass, notch and bi-quad filters). FRF analysis optimization was performed to each PID controller. The bode plots from analyzers are presented below:

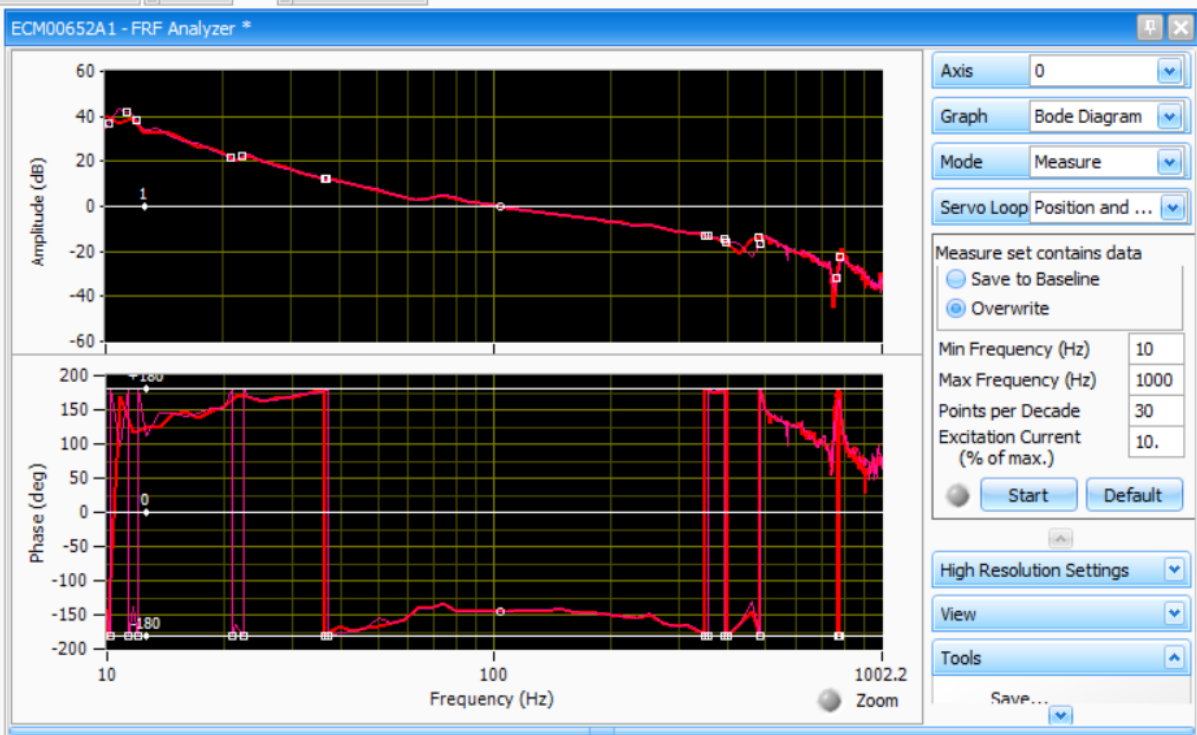


Figure 4.2 FRF bode plot PID1

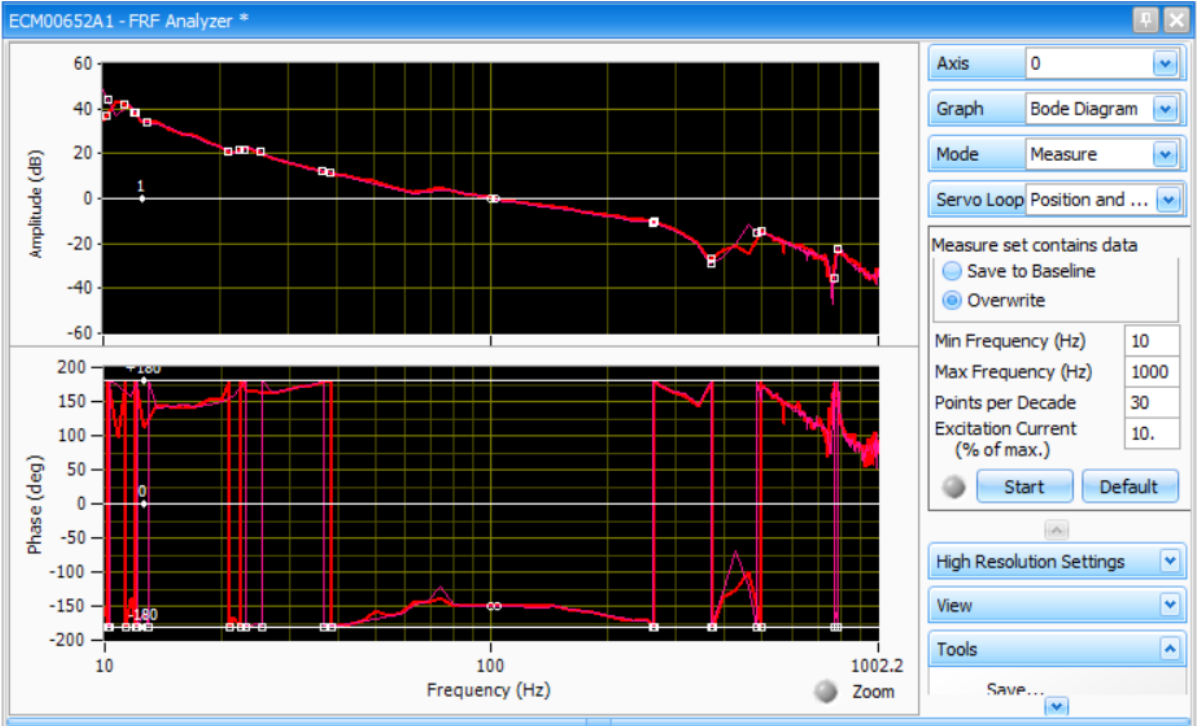


Figure 4.3 FRF bode plot PID2

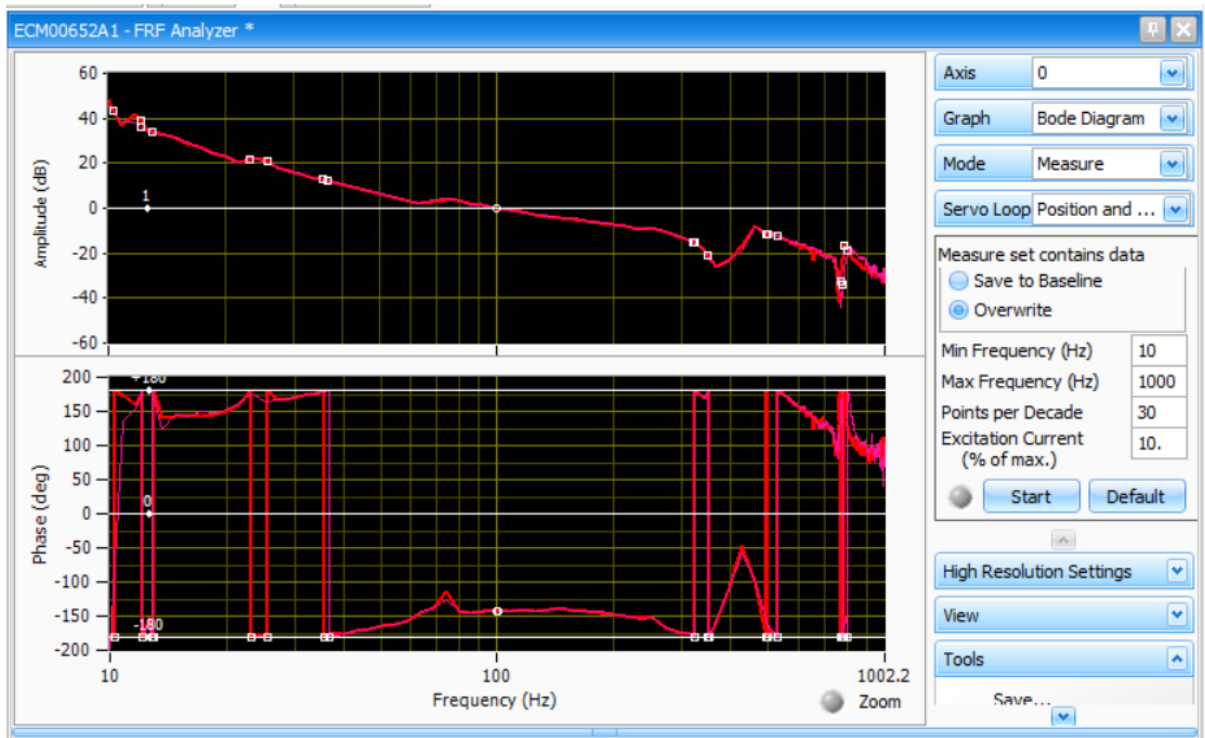


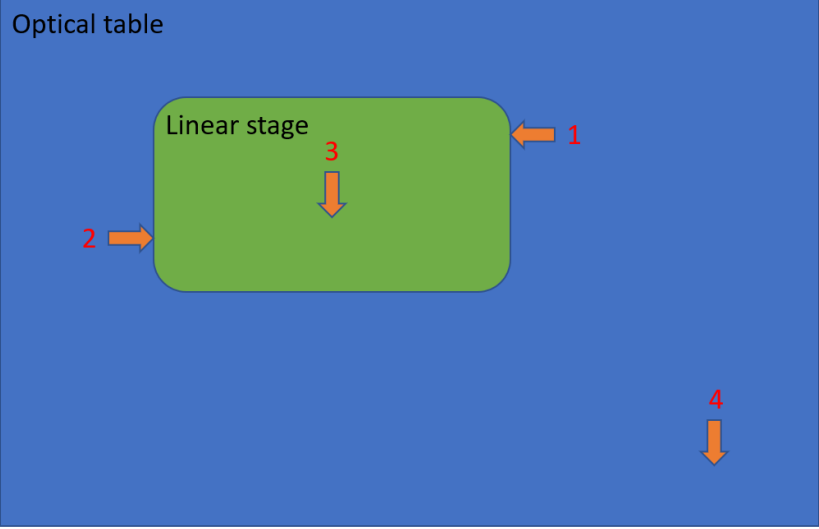
Figure 4.4 FRF bode plot PID3

Filters parameters after FRF optimization of PID controllers are provided in Table 4. Same filters parameters were used for experiments when system is affected with 1kg and 2.5kg loads.

Table 4 Parameters of PID controllers

Parameters	PID1	PID2	PID3
Position loop P coefficient	160	160	160
Velocity loop P coefficient	600	600	600
Velocity loop I coefficient	900	900	900
LPF bandwidth	500	500	500
LPF damping	0.606	0.606	0.606
NF frequency	-	370	370
NF width	-	30	30
BF denominator frequency	-	-	400
BF denominator damping	-	-	0.707
BF numerator frequency	-	-	300
BF numerator damping	-	-	0.707

Accelerometers were placed on linear stage and on optical table according to Figure 4.5 scheme. Because linear stage is made of aluminum, and accelerometers require ferromagnetic surface to mount on, steel blocks are mounted on top surface of the linear stage. 1, 2 accelerometers are mounted on the steel blocks. 3rd accelerometer is mounted on steel plate, that acts as load.



Accelerometers placements:
1, 2 – accelerometers are placed perpendicular to the linear stage X axis;
3 – accelerometer is placed perpendicular to linear stage top surface;
4 – accelerometer is placed perpendicular to optical table top surface.

Figure 4.5 Accelerometers placement scheme

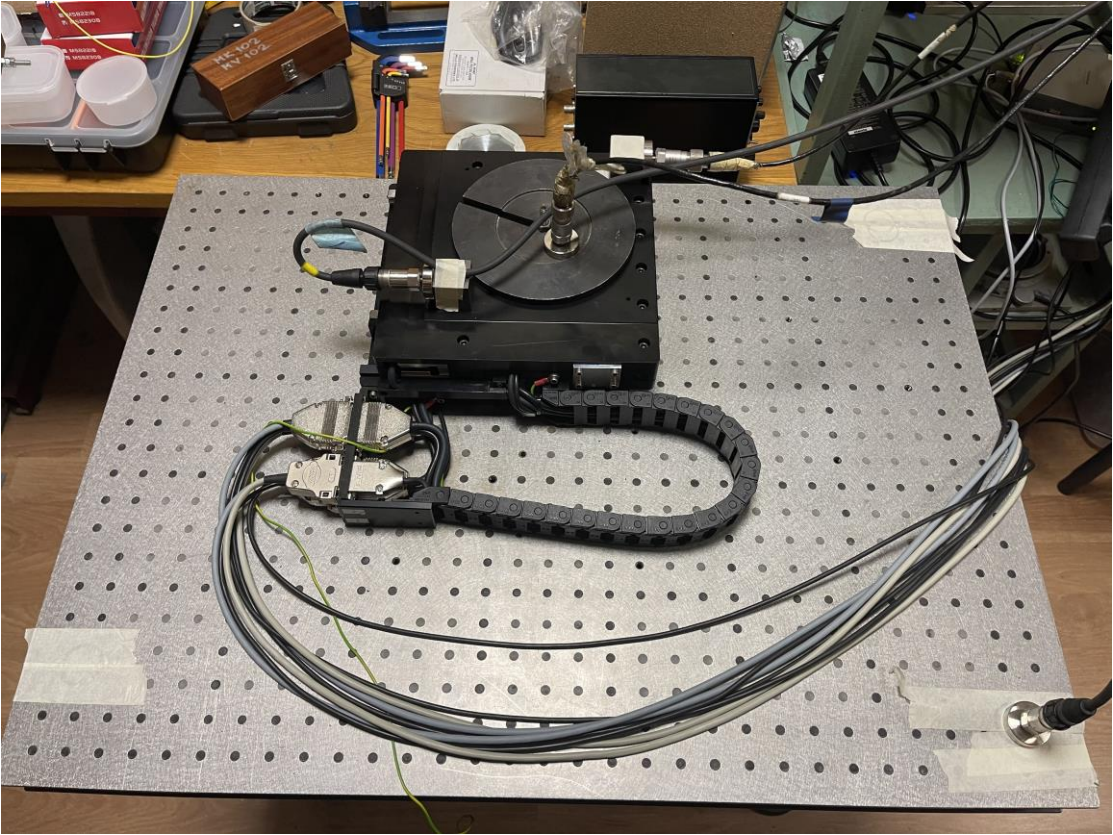


Figure 4.6 System with 1kg load

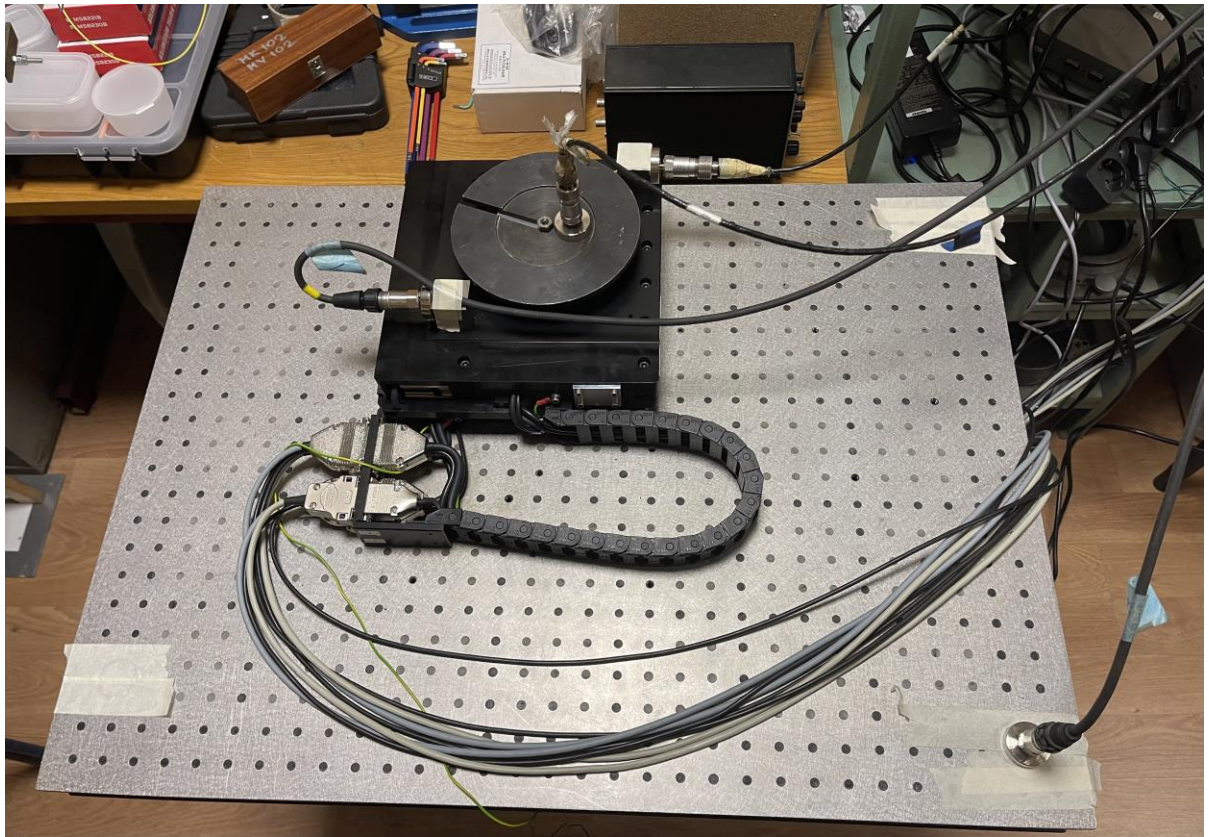


Figure 4.7 System with 2.5kg load

X axis was programmed to move at 5mm/s, 10mm/s, and 20mm/s constant velocity and with constant acceleration and deceleration. Data was collected from accelerometers and ACS controller at different velocities with different applied PID controllers, when 1kg (Figure 4.6) and 2.5kg (Figure 4.7) loads were applied at the center of linear stage moving platform.

5. Results

The data graphs acquired from accelerometers, show only the results from accelerometer numbered “1” at the Figure 4.5, which is perpendicular to the linear stage X axis.

Firstly, the system was excited by lightly striking it with the impact hammer, when the system is stationary with 1kg load applied and the motor is powered on. The results are shown in Figure 5.1. The excitation was repeated without applied filters (orange color line), when PID1 controller filters were applied (green color line), when PID2 controller filters were applied (blue color line), and when PID3 controller filters were applied (red color line).

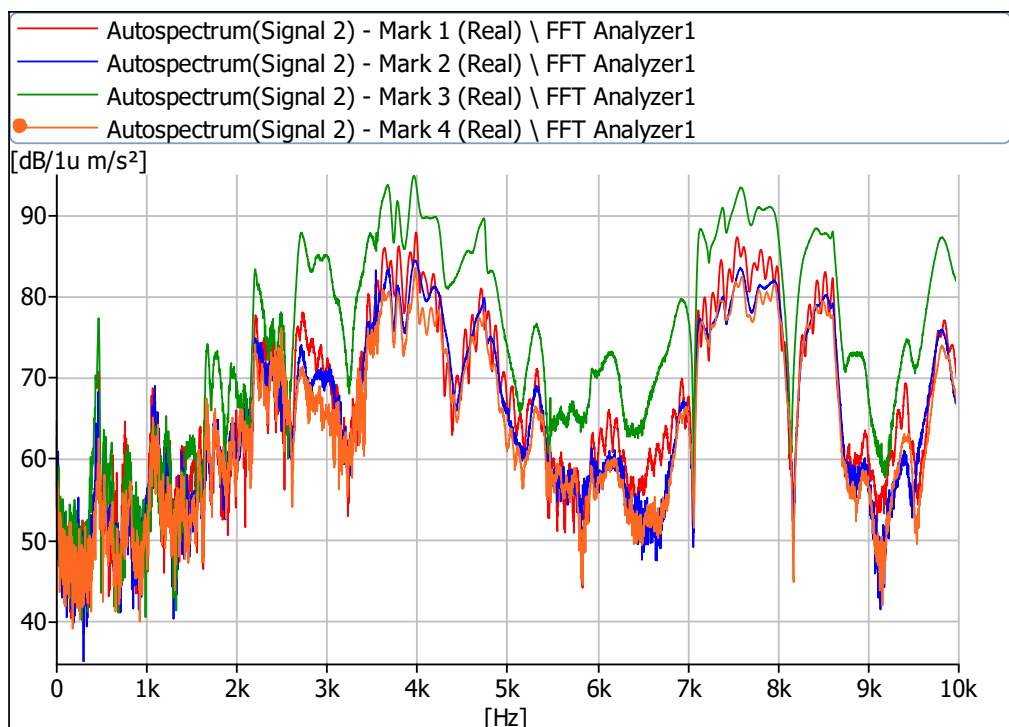


Figure 5.1 System strike excitation results when 1kg load applied

The graph shows the system amplitudes at different frequencies. The highest total amplitudes occur at low frequency range 0.1-1kHz, no matter which filters are applied. The spikes in amplitudes occur at around 500Hz, 1.1kHz, 1.7kHz, 2.2kHz, from 3.8 to 4kHz, 4.8kHz, 6kHz. Sudden drops in amplitudes occur at higher frequency range from 7-10kHz.

Due to the lower frequencies having higher total amplitudes and therefore being more damaging to the system they are more analyzed. In Figure 5.2 is shown the intensity of system amplitudes, by representing the results of system acceleration. The increase of accelerations correlates with the spikes in amplitudes. There was visible increase in accelerations at around 500Hz, 800Hz, 1.1kHz. Highest accelerations reaching around 1mm/s^2 . Accelerations are overall higher when no filters are applied, especially at 1.6-1.8kHz frequency range. The graph shows that, when PID3 controller is

applied to the system, the system produces lowest accelerations, but when PID1 controller is applied the system is most stable, the acceleration deviates the lowest.

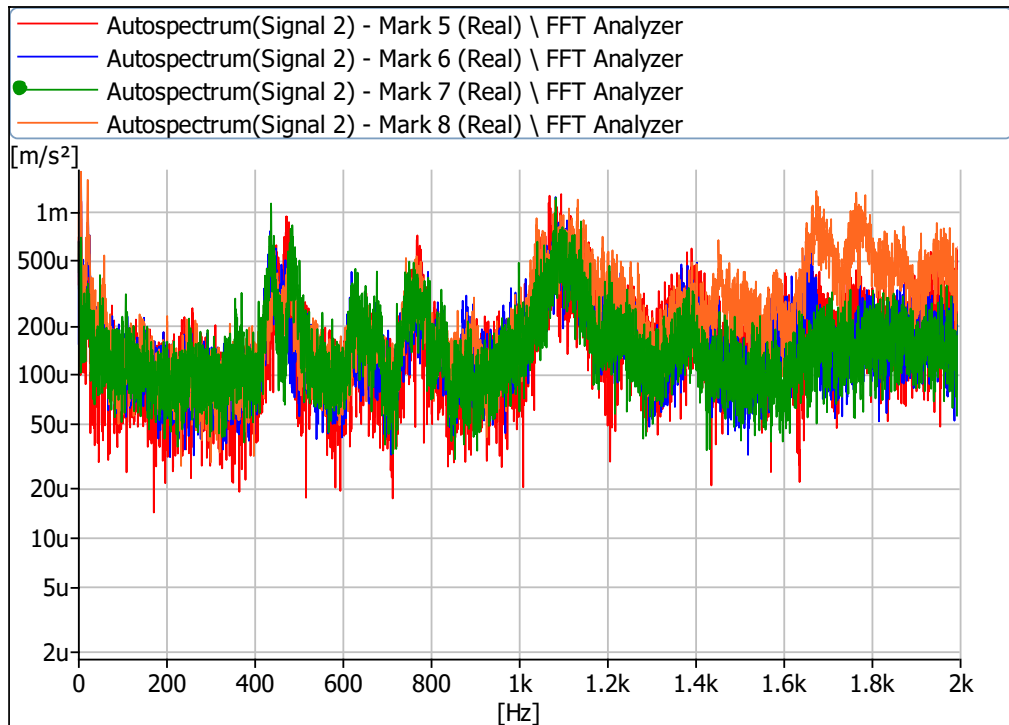


Figure 5.2 System strike excitation produced acceleration results when 1kg load is applied

After system excitation, by striking it with impact hammer, the system was excited by programming the linear stage to move at 5mm/s constant velocity and data was collected when no filters were applied (orange color line), when PID1 controller filters were applied (green color line), when PID2 controller filters were applied (blue color line), and when PID3 controller filters were applied (red color line). The results are shown in Figure 5.3.

From the graph it is seen the increase in accelerations at frequencies around 240Hz, 500Hz, 650Hz, 750Hz, 900Hz, 1.1kHz. Highest accelerations were around 1.5mm/s². PID1 controller produced highest accelerations at frequencies 500Hz, 1.1kHz and caused additional spike in acceleration at 1kHz. PID3 controller produces highest acceleration deviations and overall highest total amplitudes at all analyzed frequencies. PID2 controller produced most stable results, when applied to the system. At resonance frequencies the accelerations were the lowest and it did not produce any additional spikes in accelerations.

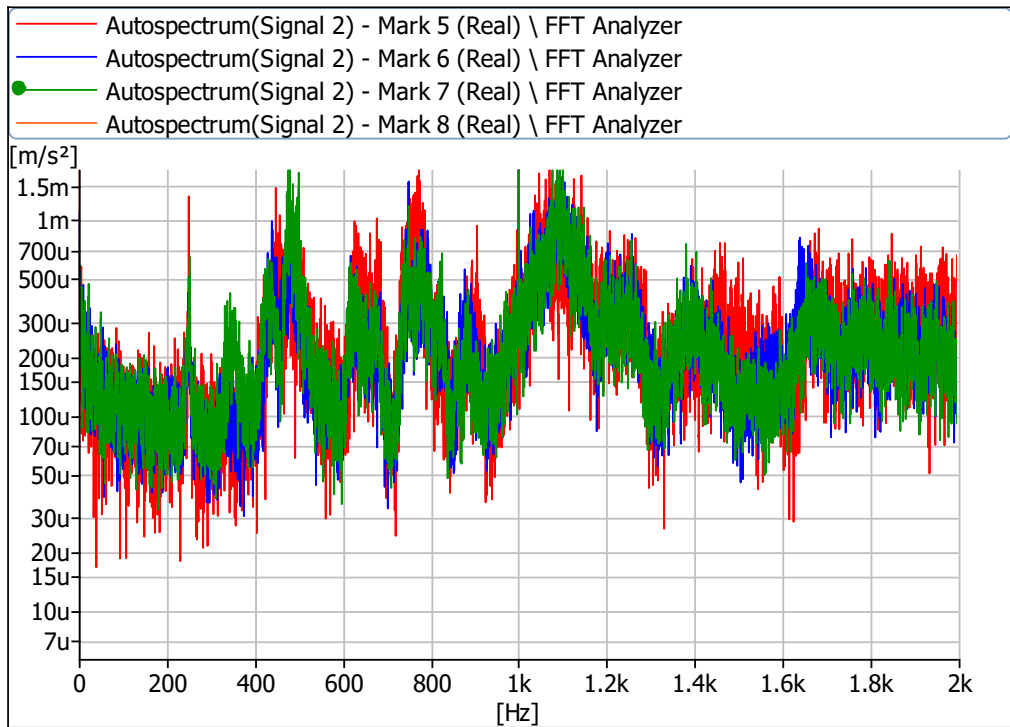


Figure 5.3 System results when 1kg load applied at 5mm/s velocity

After this, the system was excited by programming the linear stage to move at 10mm/s constant velocity and data was collected when no filters were applied (orange color line), when PID1 controller filters were applied (green color line), when PID2 controller filters were applied (blue color line), and when PID3 controller filters were applied (red color line). The results are shown in Figure 5.4.

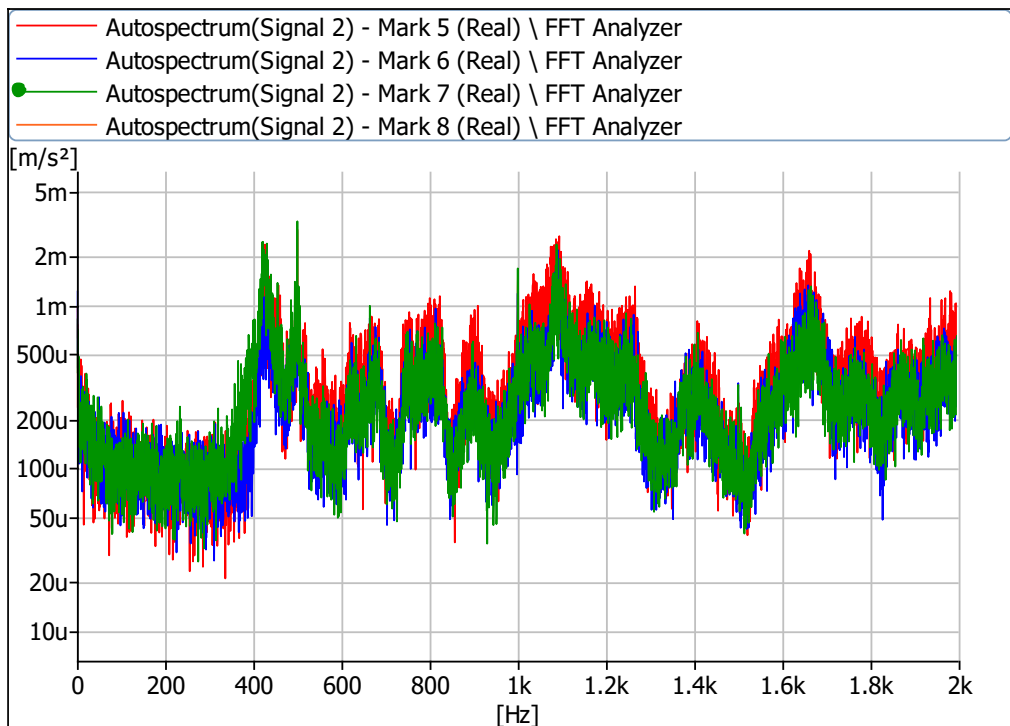


Figure 5.4 System results when 1kg load applied at 10mm/s velocity

From the graph it is seen the increase in accelerations at frequencies around 430Hz, 640-680Hz, 750-820Hz, 900Hz, 1.1kHz, 1.4kHz and 1.7kHz. Highest acceleration amplitudes were around 2mm/s². PID1 controller caused additional spike at 500Hz, but this time the total acceleration deviations were lower. PID3 controller still produced highest amplitude deviations and overall highest total amplitudes at all analyzed frequencies. PID2 controller produced most stable results, when applied to the system. At resonance frequencies the accelerations were the lowest and it did not produce any additional spikes in accelerations.

Lastly, the system was excited by programming the linear stage to move at 20mm/s constant velocity and data was collected when no filters were applied (orange color line), when PID1 controller filters were applied (green color line), when PID2 controller filters were applied (blue color line), and when PID3 controller filters were applied (red color line). The results are shown in Figure 5.5.

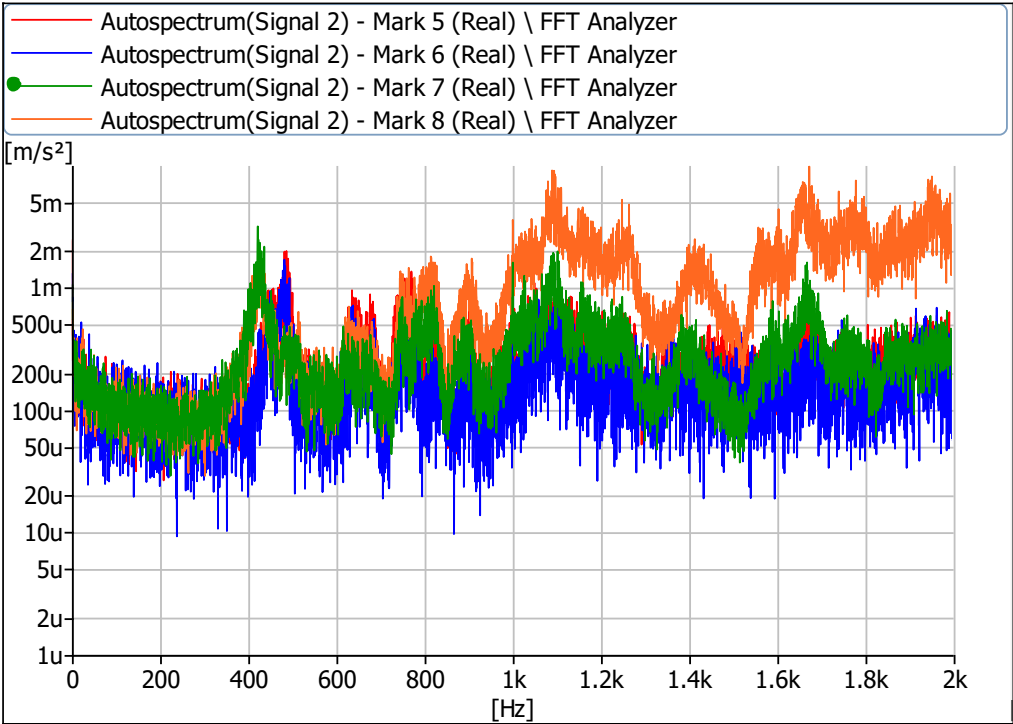


Figure 5.5 System results when 1kg load applied at 20mm/s velocity

From the graph it is seen that PID1 controller caused spike (around 2mm/s²) in accelerations at 400Hz range. PID2 controller operated at lower accelerations, but with highest deviations. And with PID3 controller produced spike at around 500Hz. The PID3 controller was the most stable.

Also, from the graph it is seen high increase in accelerations (around 5mm/s²) when no filters were applied at 0.7-2kHz frequency range. When results of accelerations at time interval (Figure 5.6) were analyzed, it was seen that accelerations when system was operating without filters dominated the graph. These high amplitudes in acceleration produces high noise and the system becomes

unusable. Therefore, the controllers must be used to achieve usable system operation conditions at higher velocities.

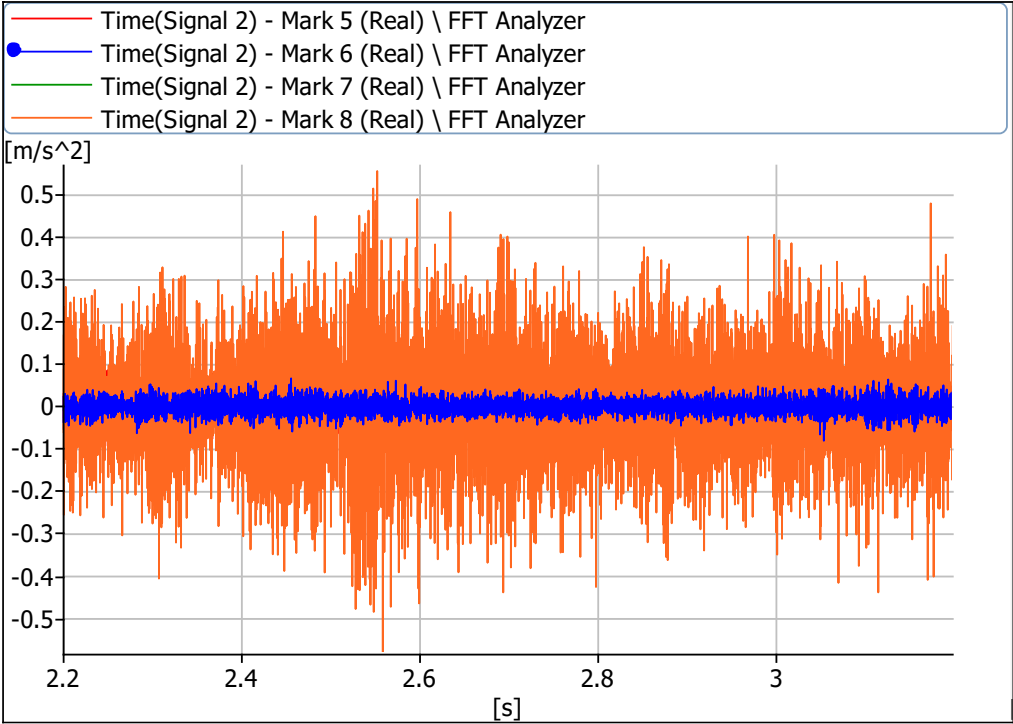


Figure 5.6 System accelerations at time interval

After experiments with 1kg of load, all experiments were repeated with the 2.5kg load applied at the same position.

The system was excited by lightly striking it with the impact hammer, when the system is stationary with 2.5kg load applied and the motor is powered. The results are shown in Figure 5.7. The excitation was repeated without applied filters (orange color line), when PID1 controller filters were applied (green color line), when PID2 controller filters were applied (blue color line), and when PID3 controller filters were applied (red color line).

The graph shows an increase in frequency amplitudes. Lowest frequencies still produce the highest total amplitudes at 0-1.5kHz. Resonant frequencies occur at 440Hz, 500Hz, 800Hz, 1.1kHz, 1.5kHz, 3.8kHz, 7.5kHz. Without filters system tends to resonate more and produce higher amplitudes. PID3 controller tends to produce high frequency amplitudes. The most stable was PID1 controller, but PID2 controller was not far from it.

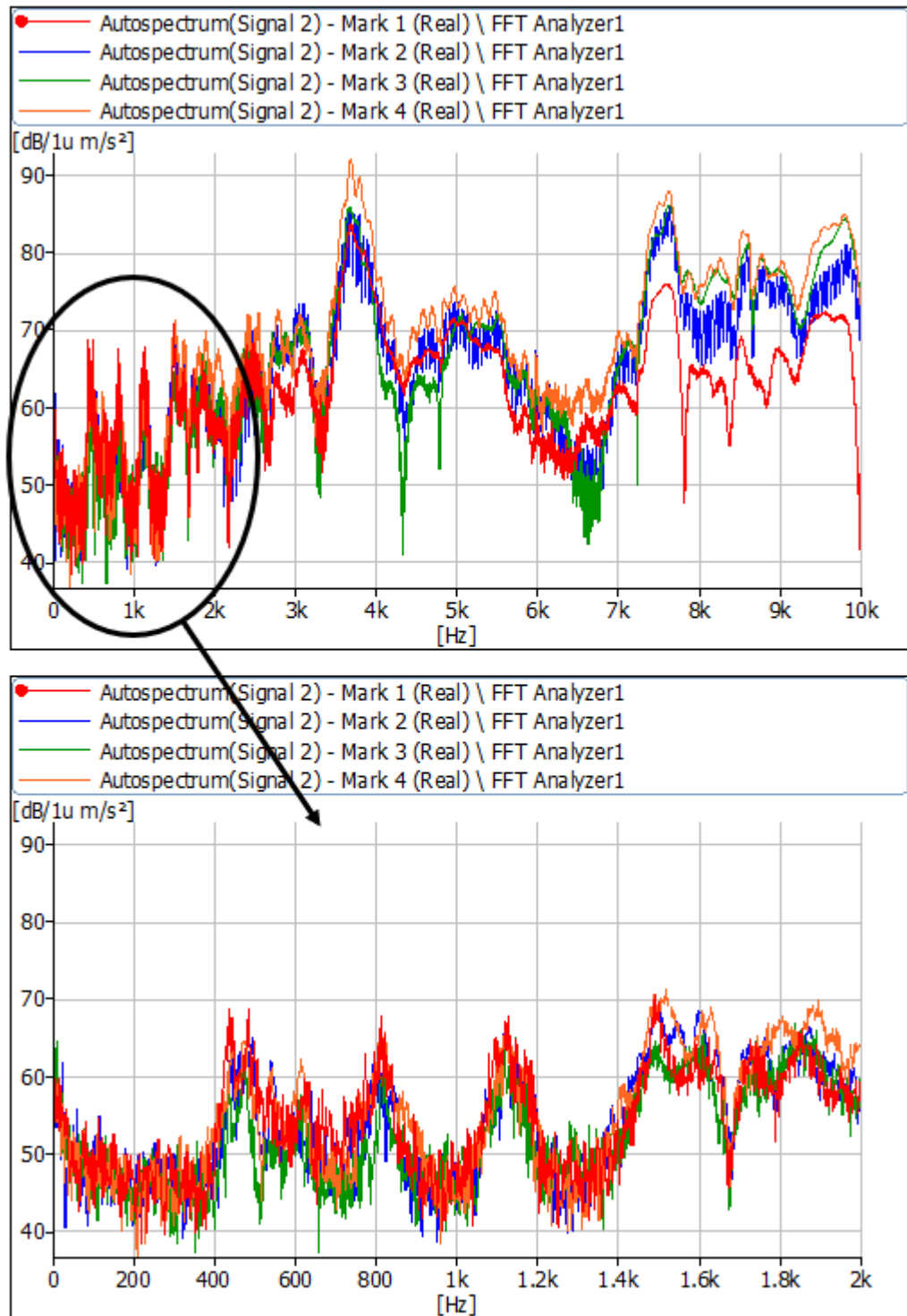


Figure 5.7 System strike excitation results when 2.5 kg load applied

After system excitation, by striking it with impact hammer, the system was excited by programming the linear stage to move at 5mm/s constant velocity and data was collected when no filters were applied (orange color line), when PID1 controller filters were applied (green color line), when PID2 controller filters were applied (blue color line), and when PID3 controller filters were applied (red color line). The results are shown in Figure 5.8.

From the graph it is seen the increase in accelerations at frequencies around 300Hz, 500Hz, 800Hz, 1.1kHz, 1.5kHz and 1.7kHz. Highest accelerations were around 2mm/s^2 . PID1 controller damped frequencies at around 300Hz, 500Hz and 1kHz that were seen when no filters were applied to the system. PID2 controller damped frequency at 300Hz, but increased system accelerations at 500Hz and 1kHz frequencies over 2mm/s^2 . Overall, PID2 controller produced lowest total amplitudes in system acceleration. PID3 controller performed poorly. It caused additional acceleration spikes at 1.6-2kHz frequency range and had higher total acceleration amplitudes in general.

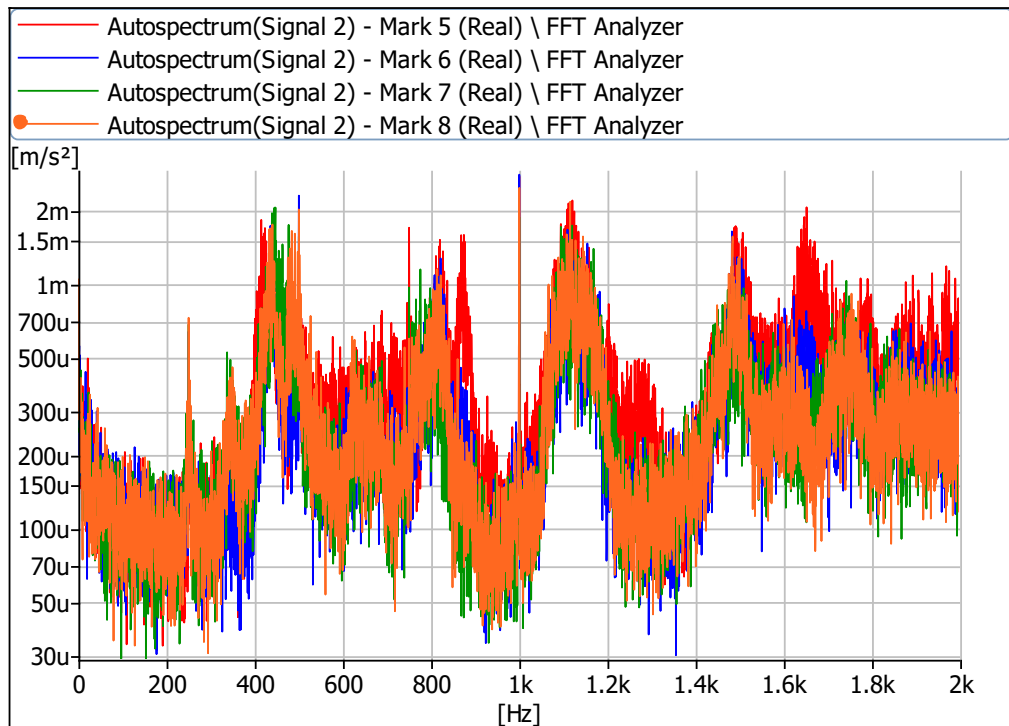


Figure 5.8 System results when 2.5kg load applied at 5mm/s velocity

After this, the system was excited by programming the linear stage to move at 10mm/s constant velocity and data was collected when no filters were applied (orange color line), when PID1 controller filters were applied (green color line), when PID2 controller filters were applied (blue color line), and when PID3 controller filters were applied (red color line). The results are shown in Figure 5.9.

From the graph it is seen the increase in accelerations at frequencies around 430-520Hz, 700Hz, 800Hz, 1.1kHz, 1.5kHz. Highest acceleration amplitudes were around 5mm/s^2 at 900Hz and 1.5kHz. PID1 controller amplified system accelerations at around 430Hz and 1.5kHz and system operated at higher acceleration overall, compared to PID2 controller and when no filters were applied results. PID2 controller operated at lower total amplitudes and produced stable results at whole analyzed frequency range 0-2kHz. PID3 controller amplified almost all resonant frequencies and produced highest total acceleration amplitudes at whole analyzed frequency range.

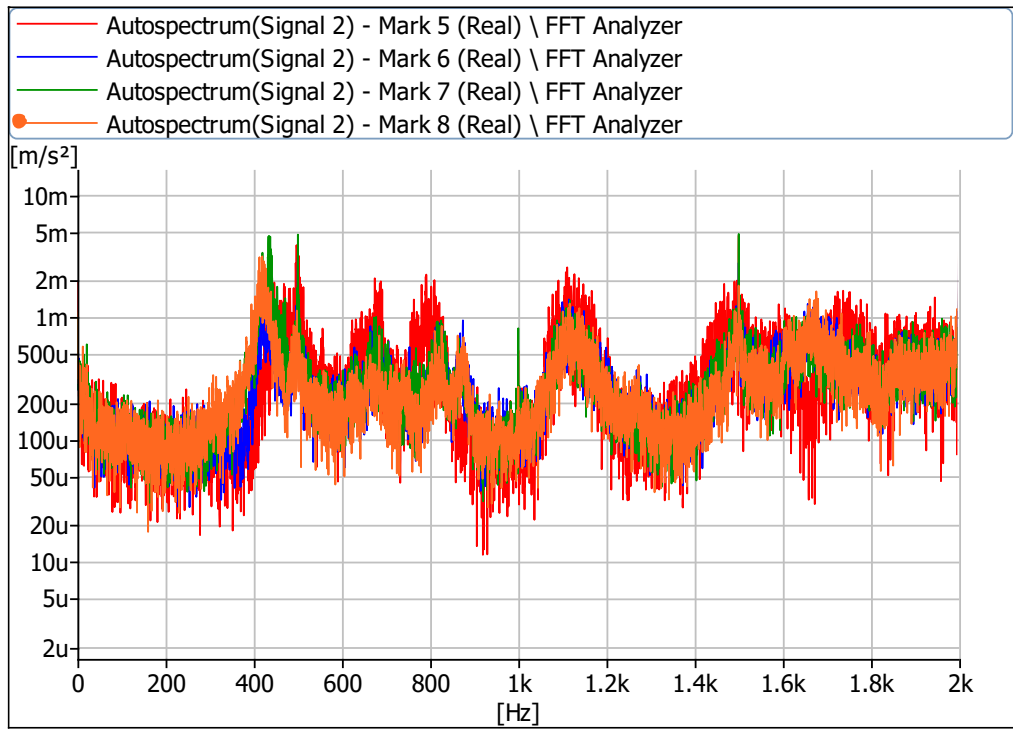


Figure 5.9 System results when 2.5kg load applied at 10mm/s velocity

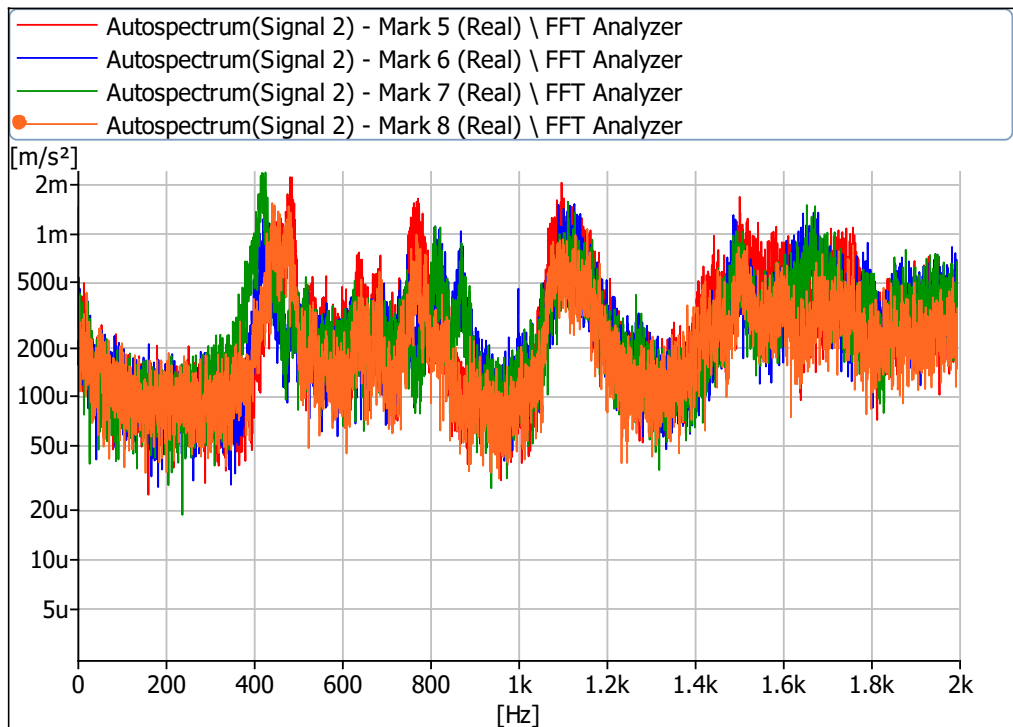


Figure 5.10 System results when 2.5kg load applied at 20mm/s velocity

Lastly, the system was excited by programming the linear stage to move at 20mm/s constant velocity and data was collected when no filters were applied (orange color line), when PID1 controller filters were applied (green color line), when PID2 controller filters were applied (blue color line), and when PID3 controller filters were applied (red color line). The results are shown in Figure 5.10.

The graph shows, that system resonance frequencies were at 400Hz, when PID1 controller was applied, and around 500Hz, 750Hz, 1.1kHz, 1.5kHz and 1.7kHz. Highest accelerations were around 1.5-2mm/s². PID1 controller produced increased accelerations at resonance frequencies and caused higher system accelerations overall. When PID3 controller was used, the system accelerations were more stable, compared to previous results at 5 and 10mm/s, but the controller amplified the acceleration amplitudes at 500Hz and 750Hz. PID2 controller operated at lowest total accelerations.

Additionally, positioning errors results were acquired from “ACS SiiPlus” software. Positioning errors were determined by linear stage encoder. Data was collected at different velocities and applied loads to the system, and positioning errors were shown at frequency range 0-1kHz.

The Figure 5.11 shows the positioning errors when 1kg load was applied to the system, and system was moving at constant 5mm/s velocity.

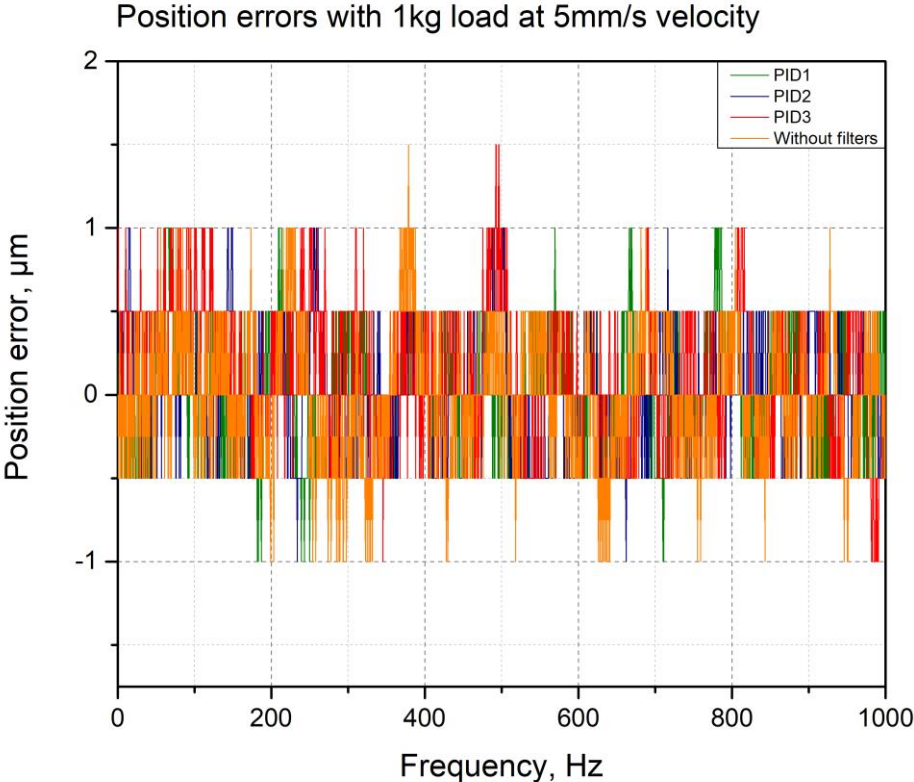


Figure 5.11 Positioning errors at 1kg load at 5mm/s velocity

Positioning errors without filters amplitudes deviates from -0.5µm to 0.5µm, with spikes reaching 1-1.5µm positioning error. But the positioning errors occur more frequently compared to when PID controllers were applied to the system. PID1 controller caused spikes of 1µm, around 200Hz and 700Hz. PID3 controller were not able to dampen the resonant frequencies of 0-200Hz range and produced significant error of 1.5µm at 500Hz resonant frequency. PID2 controller performed the best

out of all analyzed controllers. Dampening almost all resonant frequencies effects on linear stage accuracy. Producing few $1\mu\text{m}$ positioning errors at 0-200Hz frequency range and one spike at 700Hz. But overall produced less deviations, compared to other analyzed PID controllers.

The Figure 5.12 shows the positioning errors when 1kg load was applied to the system, and system was moving at constant 10mm/s velocity.

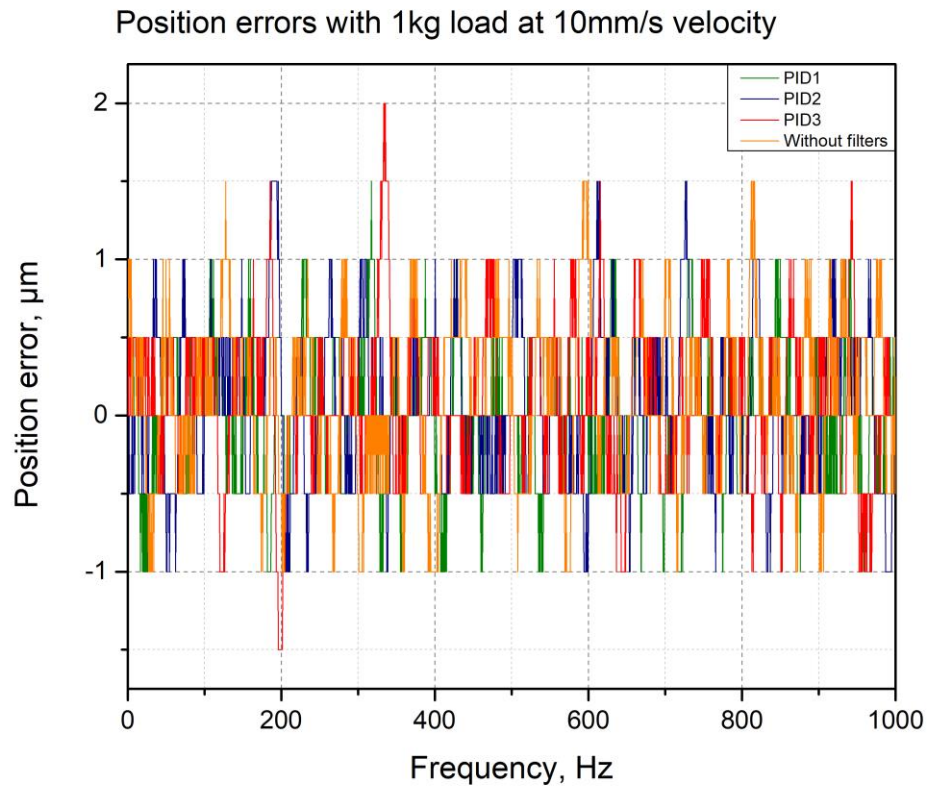


Figure 5.12 Positioning errors at 1kg load at 10mm/s velocity

Increased velocity lead to increase in overall positioning errors deviation from $[-0.5;0.5]\mu\text{m}$ to $[-1;1]\mu\text{m}$. Without filters results show the increase in positioning errors amplitude and spikes at around 170Hz, 600Hz and 810Hz frequencies. PID1 controller produced best results, by causing only one spike at around 300Hz, reaching $1.5\mu\text{m}$. PID2 controller produced several spikes at 200Hz, 600Hz and 700Hz reaching $1.5\mu\text{m}$, therefore it was second best. And PID3 controller produced worst results, by causing several spikes reaching $1.5\mu\text{m}$ and one spike in position error caused $2\mu\text{m}$ positioning error at around 320Hz frequency. All controllers reduced the frequency of positioning error happening in the system.

The Figure 5.13 shows the positioning errors when 1kg load was applied to the system, and system was moving at constant 20mm/s velocity.

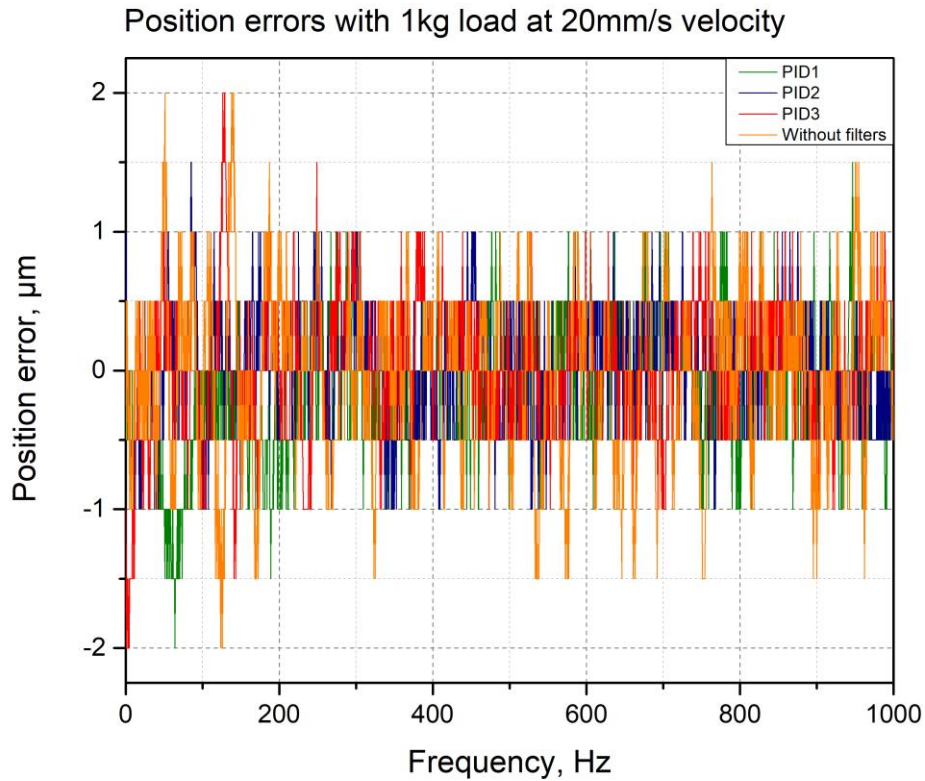


Figure 5.13 Positioning errors at 1kg load at 20mm/s velocity

When system was travelling without applied controllers, it experienced a lot of positioning errors. Several of those errors were around $2\ \mu\text{m}$ at frequencies range 0-200Hz. At that frequency range, and overall, best performed the PID2 controller. It kept position errors deviations at $[-1; 1]\ \mu\text{m}$ range, with most positioning errors at frequencies above 500Hz deviating at $[-0.5; 0.5]\ \mu\text{m}$ range. PID1 and PID3 controllers were not able to reduce positioning errors at 0-200Hz range and even introduced several new spikes. But at frequencies above 200Hz were able to keep positioning error deviations at $[-1; 1]\ \mu\text{m}$ range and eliminate spikes in positioning errors that were visible when system was without applied filters.

The Figure 5.14 shows the positioning errors when 2.5kg load was applied to the system, and system was moving at constant 5mm/s velocity.

It is seen that the frequency of positioning error occurring has increased with increased load when the system was travelling without any filters applied. Highest spikes in positioning errors increased to $2\text{-}4\ \mu\text{m}$. Also, spikes became wider, meaning, that the positioning errors persisted in wider ranges of frequencies. Applied PID controllers managed to reduce dynamic effects of linear stage and kept maximum positioning errors at $[-1.5; 1.5]\ \mu\text{m}$ ranges expect for $6\ \mu\text{m}$ positioning error produced by PID3 controller at around 200Hz and overcorrection, which lead to $2\ \mu\text{m}$ positioning error afterwards

and caused system oscillation. Overall positioning errors deviated at $[-0.5;0.5]\mu\text{m}$ range with occasional increase to $[-1;1]\mu\text{m}$ range. PID2 caused increase in positioning error at around 500Hz, with positioning errors persisting for wider frequency ranges. While PID1 controller produced few smaller spikes at around 150Hz and 800Hz, therefore making the PID1 controller performance the most stable at 5mm/s velocity.

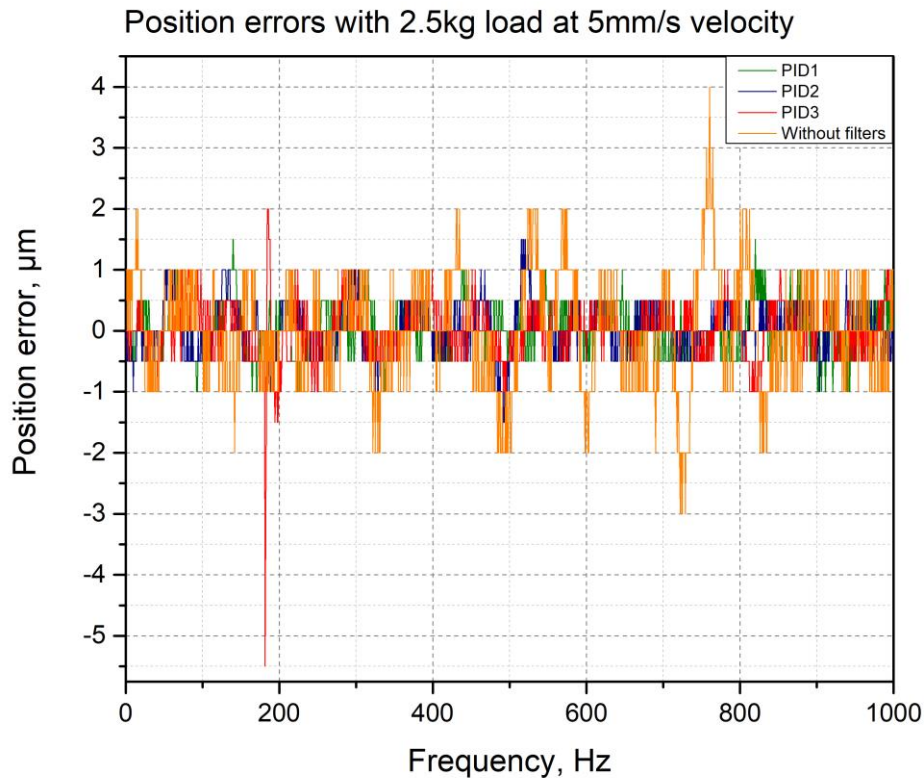


Figure 5.14 Positioning errors at 2.5kg load at 5mm/s velocity

The Figure 5.15 shows the positioning errors when 2.5kg load was applied to the system, and system was moving at constant 10mm/s velocity.

The graph shows increased positioning errors frequency and values with wider spike at around 400Hz and positioning error value of $3.5\mu\text{m}$ and smaller spike at 500Hz with value of $3\mu\text{m}$, when system was without applied filters. PID1 controller caused spikes at around 400Hz and 750Hz with 2 and $1.5\mu\text{m}$ positioning error values. PID2 controller more frequently produced positioning errors and produced a wide error spike at 900-950Hz range with highest value of $2.5\mu\text{m}$. PID3 controller produced most stable results. It eliminated the most positioning errors and the majority of produced positioning errors values deviated at $[-0.5;0.5]\mu\text{m}$ range, with small spikes at around 800Hz and 900Hz.

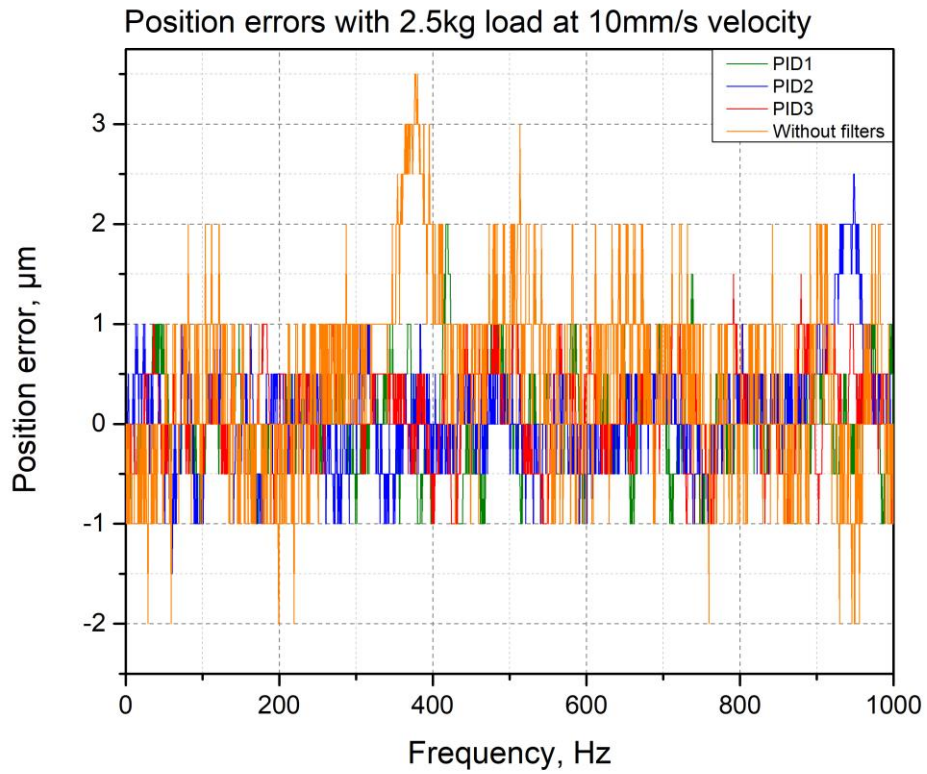


Figure 5.15 Positioning errors at 2.5kg load at 10mm/s velocity

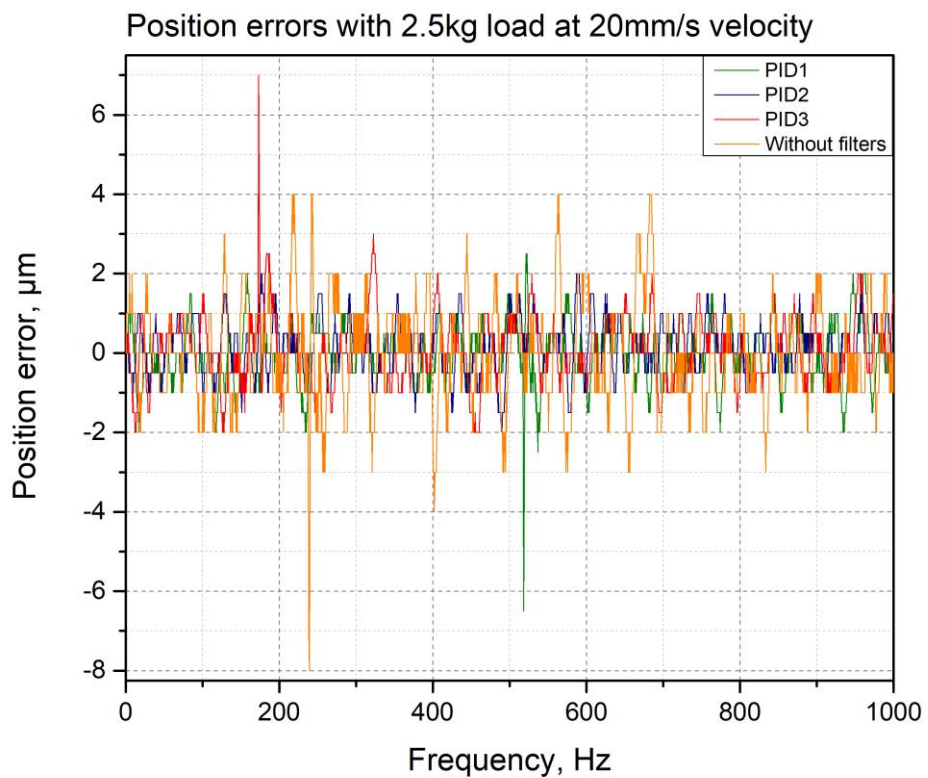


Figure 5.16 Positioning errors at 2.5kg load at 20mm/s velocity

The Figure 5.16 shows the positioning errors when 2.5kg load was applied to the system, and system was moving at constant 20mm/s velocity.

Increased velocity resulted in increase in positioning errors values. Linear stage moving without applied filters produced several spikes with values deviating at $[-8;4]\mu\text{m}$ range. $8\mu\text{m}$ positioning error occurred at around 200Hz, and the system kept oscillating through all analyzed frequency range with peaks and valleys of positioning errors deviating at $[-4;4]\mu\text{m}$ values. PID3 controller caused spike in positioning error at around 200Hz with positioning error value of $7\mu\text{m}$. After this, the positioning error values deviated at $[-2;2]\mu\text{m}$ range. PID1 controller caused an oscillation in positioning errors at 500-600Hz with spike of $6.5\mu\text{m}$. But the overall positioning error values were more stable compared to PID3 controller. PID2 controller produced best results for linear stage accuracy. It eliminated most of the positioning errors and occurred error values deviated from $-1.5\mu\text{m}$ to $1.5\mu\text{m}$.

Conclusions

Analysis of scientific papers and experiments were done. All gathered data was considered and according to it the theoretical and experimental analysis with methodology was written.

In master thesis, modal analysis of the research object was performed, and five modes that show deformations of X axis were obtained. Theoretically obtained mode frequencies were 446 Hz, 1723 Hz, 2254 Hz, 3945 Hz and 5934 Hz. Experimentally obtained resonant frequencies were around 500 Hz, 1.7 kHz, 2.2 kHz, 3.8 kHz and 6 kHz. Theoretical analysis results were approximately 89-99% accurate to real life conditions. Therefore, theoretical results were determined to be satisfactory and suitable for use.

The practical experiment showed that the highest total amplitudes in the system occur at low frequencies and have the biggest effect on linear stage accuracy, especially at 0-200 Hz range.

Also, practical experiment showed, that PID controller architecture effectiveness depends on the applied load and velocities. When lower loads were applied to the system, PID controller importance was mostly seen in analyzed higher velocities, where applied controllers reduced the noise of the system and positioning error values from 0.5-2 μm to 0.5-1 μm or eliminated positioning errors completely, compared to the results, where no filters were applied to the system. When system was under higher loads, controllers had a huge effect on linear system positioning accuracy at all analyzed velocities, where applied controllers reduced positioning error values from 0.5-8 μm to 0.5-1.5 μm , compared to the results, where no filters were applied to the system.

It is recommended to use PID2 controller architecture for overall use of the linear stage, because it produced most stable results at low and high velocities under small and heavy applied loads. PID1 controller architecture is recommended to use at medium velocities under small loads or at low velocities under heavy loads. PID3 controller architecture is recommended to use at medium velocities under heavy loads.

References

- [1] K. Sato and T. Hama, "High-speed positioning of ultrahigh-acceleration and high-velocity linear synchronous motor," *Int. J. Precis. Eng. Manuf.*, vol. 15, no. 8, pp. 1537–1544, 2014, doi: 10.1007/s12541-014-0502-y.
- [2] M. Salman, "Analysis, design and control aspects of linear machines using co-simulation," 2012.
- [3] J. Rigelsford, "Linear Synchronous Motors: Transportation and Automation Systems," *Assem. Autom.*, vol. 20, no. 3, p. 3, 2000, doi: 10.1108/aa.2000.03320cad.017.
- [4] K. M. Tao, R. L. Kosut, and G. Aral, "Learning feedforward control," *Proc. Am. Control Conf.*, vol. 3, no. 3, pp. 2575–2579, 1994, doi: 10.1109/acc.1994.735024.
- [5] A. Najjar-Khodabakhsh and J. Soltani, "MTPA control of mechanical sensorless IPMSM based on adaptive nonlinear control," *ISA Trans.*, vol. 61, pp. 348–356, 2016, doi: 10.1016/j.isatra.2016.01.004.
- [6] S. Madanzadeh, A. Abedini, A. Radan, and J. S. Ro, "Application of quadratic linearization state feedback control with hysteresis reference reformer to improve the dynamic response of interior permanent magnet synchronous motors," *ISA Trans.*, vol. 99, no. xxxx, pp. 167–190, 2020, doi: 10.1016/j.isatra.2019.08.067.
- [7] C. Cavallaro, A. O. Di Tommaso, R. Miceli, A. Raciti, G. R. Galluzzo, and M. Trapanese, "Efficiency enhancement of permanent-magnet synchronous motor drives by online loss minimization approaches," *IEEE Trans. Ind. Electron.*, vol. 52, no. 4, pp. 1153–1160, 2005, doi: 10.1109/TIE.2005.851595.
- [8] H. Eldeeb, C. M. Hackl, L. Horlbeck, and J. Kullick, "A unified theory for optimal feedforward torque control of anisotropic synchronous machines," *Int. J. Control*, vol. 91, no. 10, pp. 2273–2302, 2018, doi: 10.1080/00207179.2017.1338359.
- [9] X. Liu, Q. Liu, and W. Fu, "Optimal design of permanent magnet arrangement in synchronous motors," *Energies*, vol. 10, no. 11, 2017, doi: 10.3390/en10111700.
- [10] A. Pizarro-Lerma, V. Santibañez, R. Garcia-Hernandez, and J. Villalobos-Chin, *Sectorial fuzzy controller plus feedforward for the trajectory tracking of robotic arms in joint space*, vol. 9, no. 6. 2021.
- [11] A. G. M. A. Aziz, H. Rez, and A. A. Zaki Diab, "Robust sensorless model-predictive torque flux control for high-performance induction motor drives," *Mathematics*, vol. 9, no. 4, pp. 1–29, 2021, doi: 10.3390/math9040403.
- [12] A. Piščalov, E. Urbonas, N. Višniakov, D. Zabulionis, and A. Kilikevičius, "Investigation of position and velocity stability of the nanometer resolution linear motor stage with air bearings by shaping of controller transfer function," *Symmetry (Basel)*, vol. 12, no. 12, pp. 1–16, 2020, doi: 10.3390/sym12122062.
- [13] B. Qu, Q. Yang, Y. Li, M. A. Sotelo, S. Ma, and Z. Li, "A novel surface inset permanent magnet synchronous motor for electric vehicles," *Symmetry (Basel)*, vol. 12, no. 1, 2020, doi: 10.3390/SYM12010179.
- [14] S. Komada, M. Ishida, T. Hori, and K. Ohnishi, "Disturbance observer-based motion control of direct drive motors," *IEEE Trans. Energy Convers.*, vol. 6, no. 3, pp. 553–559, 1991, doi: 10.1109/60.84334.
- [15] J. Wu, Z. Xiong, K. M. Lee, and H. Ding, "High-acceleration precision point-to-point motion

- control with look-ahead properties,” *IEEE Trans. Ind. Electron.*, vol. 58, no. 9, pp. 4343–4352, 2011, doi: 10.1109/TIE.2010.2098363.
- [16] R. Cao and K. S. Low, “A repetitive model predictive control approach for precision tracking of a linear motion system,” *IEEE Trans. Ind. Electron.*, vol. 56, no. 6, pp. 1955–1962, 2009, doi: 10.1109/TIE.2008.2007034.
- [17] P. H. Chou, F. J. Lin, C. S. Chen, and F. C. Lee, “DSP-based cross-coupled synchronous control for dual linear motors via intelligent complementary sliding mode control,” *CHUSER 2012 - 2012 IEEE Colloq. Humanit. Sci. Eng. Res.*, vol. 59, no. 2, pp. 266–271, 2012, doi: 10.1109/CHUSER.2012.6504322.
- [18] Z. Chen, B. Yao, and Q. Wang, “ μ -synthesis-based adaptive robust control of linear motor driven stages with high-frequency dynamics: A case study,” *IEEE/ASME Trans. Mechatronics*, vol. 20, no. 3, pp. 1482–1490, 2015, doi: 10.1109/TMECH.2014.2369454.
- [19] RAYEX ELEC., “Lm Series,” *Rayex Elec.*, p. 2, 2014, [Online]. Available: <https://datasheet.octopart.com/LM2-9D-Rayex-datasheet-36985588.pdf>.
- [20] X. Liu, J. Gao, S. Huang, and K. Lu, “Magnetic Field and Thrust Analysis of the U-Channel Air-Core Permanent Magnet Linear Synchronous Motor,” *IEEE Trans. Magn.*, vol. 53, no. 6, pp. 2015–2018, 2017, doi: 10.1109/TMAG.2017.2655082.
- [21] N. A. Mohd Nasir, F. A. bin Abdul Shukor, R. N. Firdaus, H. Wakiwaka, K. Tashiro, and M. Nirei, “Design of the permanent magnet linear synchronous motor for high thrust and low cogging force performance,” *Prog. Electromagn. Res. M*, vol. 63, no. January, pp. 83–92, 2018, doi: 10.2528/pierm17101907.
- [22] P. Andersen, “Operational Modal Analysis,” *Operational Modal Analysis*. pp. 1–63, 2017.
- [23] “<https://eomys.com/e-nvh/technical-notes-on-electromagnetically-excited-noise-and-vibrations/article/what-is-a-frf-frequency-response-function>. [Interactive: 2021-04-11]”.
- [24] K. K. Tautvydas Pravilonis, Edgar Sokolovskij, Artūras Kilikevičius, Jonas Matijošius, “SS symmetry The Usage of Alternative Materials to Optimize Bus,” 2020.
- [25] Y. Zeqing, L. Libing, W. Zuojie, C. Yingshu, and X. Quanyang, “Static and Dynamic Characteristic Simulation of Feed System Driven by Linear Motor in High Speed Computer Numerical Control Lathe,” *TELKOMNIKA Indones. J. Electr. Eng.*, vol. 11, no. 7, pp. 3673–3683, 2013, doi: 10.11591/telkomnika.v11i7.2813.
- [26] A. Piš, E. Urbonas, D. Vainorius, and J. Matijošius, “Investigation of X and Y Configuration Modal and Dynamic Response to Velocity Excitation of the Nanometer Resolution Linear Servo Motor Stage with Quasi-Industrial Guiding System in Quasi-Stable State,” 2021.
- [27] M. A. Johnson *et al.*, *PID control: New identification and design methods*. 2005.
- [28] F. Greg Shinsky, “PID control,” *Meas. Instrumentation, Sensors Handb. Spat. Mech. Therm. Radiat. Meas. Second Ed.*, pp. 91-1-91–9, 2017, doi: 10.1201/b15474.
- [29] M. Araki, “Control system, robotics and automation,” vol. II, pp. 694–696, 2017, doi: 10.1109/icit.2017.7915443.
- [30] K. H. Ang, G. Chong, and Y. Li, “PID control system analysis, design, and technology,” *IEEE Trans. Control Syst. Technol.*, vol. 13, no. 4, pp. 559–576, 2005, doi: 10.1109/TCST.2005.847331.
- [31] A. K. Ho, “Fundamental of PID Control,” vol. 331, 2014.

- [32] “<https://www.motioncontroltips.com/faq-servo-motor-current-velocity-position-loops-bandwidths/> [Interactive: 2021-04-11].” .
- [33] “<https://www.acs-controlsystem.de/en/home/>[Interactive: 2021-04-14].” .

APPENDEXES

Appendix 1. Conference paper

INVESTIGATION OF DYNAMIC PROCESSES OF PRECISION POSITIONING SYSTEMS WITH LINEAR MOTOR

Vilius Kavaliauskas, Edgaras Urbonas, Artūras Kilikevičius

Vilniaus Gedimino technikos universitetas, Vilnius, Lietuva

Emails: vilius.kavaliauskas@stud.vgtu.lt, edgaras.urbonas@vgtu.lt, arturas.kilikevicius@vgtu.lt

Abstract

Fast-paced competition in industrial environment require high accuracy and performance systems, which allow the industry players to stay on top. The change in mechanical structure of the precision positioning system is no longer enough. Therefore, frequency domain analysis must be done. In this paper, X axis of the precision positioning system with linear motor is analyzed. The PID controllers of different architectures are investigated to determine their effect on the platform moving at three different constant velocities.

Key words: linear motor, frequency dynamics, precision positioning.

Introduction

Linear synchronous motors (LSM) offer significant advantages for precision positioning systems, where high dynamic performance is required [1]-[2]. Linear motion is transmitted without the use of intermediate gears, screws or crank shafts, but with the use of the magnetic field [3]. Therefore, linear motors do not suffer from the problems caused by the power transmission. This kind of systems are more accurate, due to less friction and no backlash, faster, more efficient, reliable and have longer lifetime, due to mechanical construction simplicity, compared to other rotary machines[1],[2],[4].

Increase of industrial demand on accuracy and speed, makes LSM positioning systems more in demand each year. Therefore, a demand for research, for this kind of systems, is high to further improve the technology. Many methods have been developed to deal with the uncertainties of LSM and significant amount of research on the dynamic processes were done. But the majority of the research is based on rigid-body dynamics of the system. The lack of research on the high-frequency dynamics have become the main limiting factor in improving linear motor driven positioning systems performance and better control [5].

In this paper, experimental research of dynamic processes of the precision positioning system with linear motor based on frequency domain is analyzed. Frequency response function (FRF) is used to determine PID controller effects on the system. No known research of the researched object has been done. Therefore, produced results could be used to improve system performance.

Research object

Research object - 8MTL120XY, a direct drive planar XY linear translation stage, which uses a pair of three phase ironless linear brushless servo motors. Direct drive technology enables linear stage to achieve zero backlash motion, resulting in high accuracy, repeatability and low friction. Used for accurate positioning of an object along a single axis.



Figure 1 8MTL120XY [6]

Similar research

Investigation of Position and Velocity Stability of the Nanometer Resolution

Linear Motor Stage with Air Bearings by Shaping of Controller Transfer Function.

The authors of this research paper analyzed the dynamic errors of the displacement of the platform of the one degree of freedom long-travel linear motor stage with air bearings by applying different controllers consisting of a low-pass (LPF), notch (NF), and second-order bi-quad (BF) filters at different velocities. The plant was excited by the frequency based sinusoidal current of the constant amplitude, while the system was moving at constant speed. The accelerometer was used to compare identified eigenfrequencies to the harmonic excitation obtained by the frequency response function (FRF) of the plant investigated. The configurations on the controllers were: PID1 (where only LPF is used), PID2 (where LPF and NF are used) and PID3 (where LPF, NF and BF are used). It was determined that higher-order controllers can reduce the dynamic error significantly at low velocities of the moving platforms: 1 and 5 mm/s. Moreover, the low order controllers of 4th-degree polynomials of the transfer function can also provide small dynamic errors of the displacement of the platform [7].

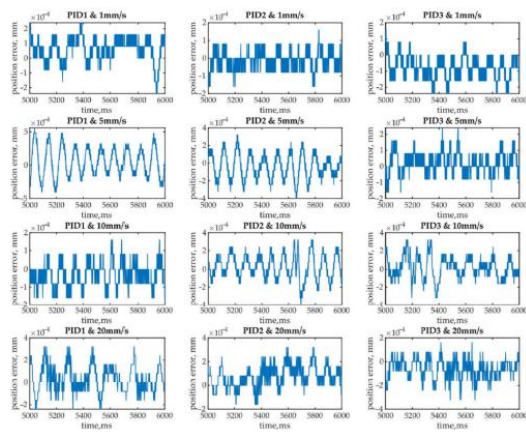


Figure 2 Dynamic displacement errors of LMS platform with different controllers at different velocities and constant acceleration [7]

Use of Accelerometer for Precision Motion Control of Linear Motor Driven Positioning System. The paper investigated the benefits of using accelerometer and additional position sensors for precision motion control of linear motor driven positioning system. The sampling rate was

chosen of 5kHz with the essential parameters summarized in Figure 8. The results showed that the use of additional sensors and accelerometers produced smoother estimates and control action of the linear motor system with less delay, when using Kalman filter, compared to using low pass filter [8].

Essential experimental parameters (sampling period=2msec)		
Parameters	Numerical Values	
State Feedback Controller	K_p	26455
	K_v	65.4545
DOB	m_s	2.7 [kg]
	$K_{a, \text{nom}}$	33 [N/V]
	$Q(s) = \frac{3\tau + 1}{(\tau s)^3 + 3(\tau s)^2 + 3(\tau s) + 1}$ $\tau = 0.3$	
Kalman Filter	$E\{a_G^2\}$	1.056
	$E\{x_G\}$	5.2×10^{-13}
Friction Compensator	f_d	0.42
	f_c	0.36

Figure 3 Essential parameters [8]

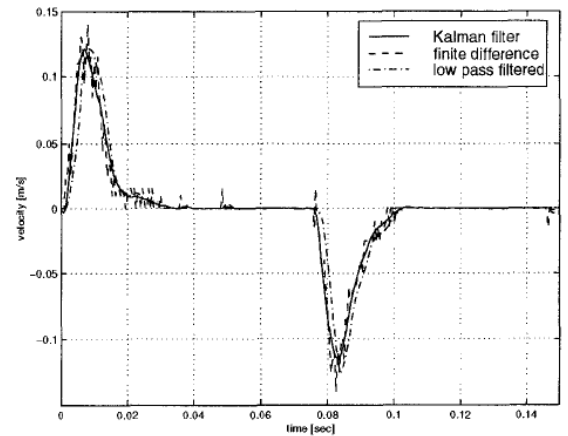


Figure 4 Comparison of velocity estimates by different methods [8]

Static and Dynamic Characteristic Simulation of Feed System Driven by Linear Motor in High-Speed Computer Numerical Control Lathe. The authors of this research paper analyzed static and dynamic characteristics of the lathes feed system driven by linear motor. It was determined that the highest deformation of the slide board occurs in the middle of the slide board where the linear motor is placed. Using MATLAB software linear motor dynamic stiffness was analyzed. The simulation results show that the position loop proportional gain, speed loop proportional gain and speed loop integral response time are the biggest influence factors on servo dynamic stiffness. The displacement response is reduced under the cutting interference force step inputting, while the

position loop proportional gain, speed loop proportional gain and speed loop integral response time are increased, and the servo dynamic stiffness is increased, the number of system oscillation is also reduced, and the system tends to be stable [9].

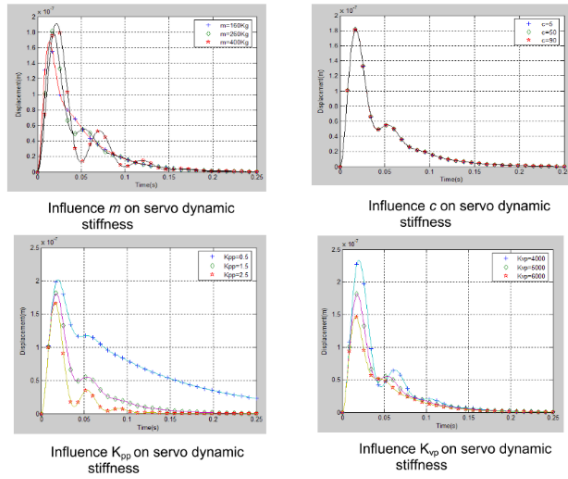


Figure 5 Influence K_{pp} (position loop proportional gain), K_{vp} (speed loop proportional gain), T_n (speed loop integral response time constant), K_{cp} (current loop gain) on servo dynamic stiffness [9]

Experiment of dynamic processes of precision positioning systems with linear motor. The importance of PID controller filters are determined by the linear stage mounting area quality, applied load, and applied load position from the center of mass.

Precision positioning system linear stage experiment setup is shown in Figure 6.



Figure 6 Experimental setup of precision positioning system with linear motor dynamic processes

Research object, 8MTL120XY a direct drive planar XY linear translation stage, is placed on the “Standa” optical table to ensure

stability. Only one axis, X axis, is used for the experiment, therefore, the Y axis is locked using provided transportation tool. Due to the linear stage being made of aluminum, steel blocks are mounted on the top of the stage by screwing them to the threaded holes. Accelerometers are then mounted on steel blocks and optical table surface. Accelerometers signal cables are connected to NI USB-4431 dynamic signal acquisition module for acquiring high-accuracy measurements, which is then connected to DELL laptop. Linear stage is connected to ACS Motion Control controller and plugged to the laptop. Using ACS SPiiPlusSC software, position and velocity loops are optimized for the best performance. After velocity and position loops optimization, three PID controller filters configurations, which provide stable linear stage operation, are applied to the linear stage controller: PID1 (low pass filter), PID2 (low-pass and notch filters), and PID3 (low-pass, notch and bi-quad filters).

Table 1 Parameters of PID controllers

Parameter	PID1	PID2	PID3
Position loop P coefficient	160	160	160
Velocity loop P coefficient	600	600	600
Velocity loop I coefficient	900	900	900
LPF bandwidth	500	500	500
LPF damping	0.606	0.606	0.606
NF frequency	-	370	370
NF width	-	30	30
BF denominator frequency	-	-	400
BF denominator damping	-	-	0.707
BF numerator frequency	-	-	300
BF numerator damping	-	-	0.707

During the experiment, the change in frequency amplitude is observed, using frequency response function (FRF), when the system is excited by the sweep of motor frequencies (from 10Hz to 10kHz). Linear stage is programmed to move at different constant velocities (5mm/s; 10mm/s; 20mm/s) with constant acceleration, and three PID

controllers are applied one at a time. Data is collected from the accelerometers.

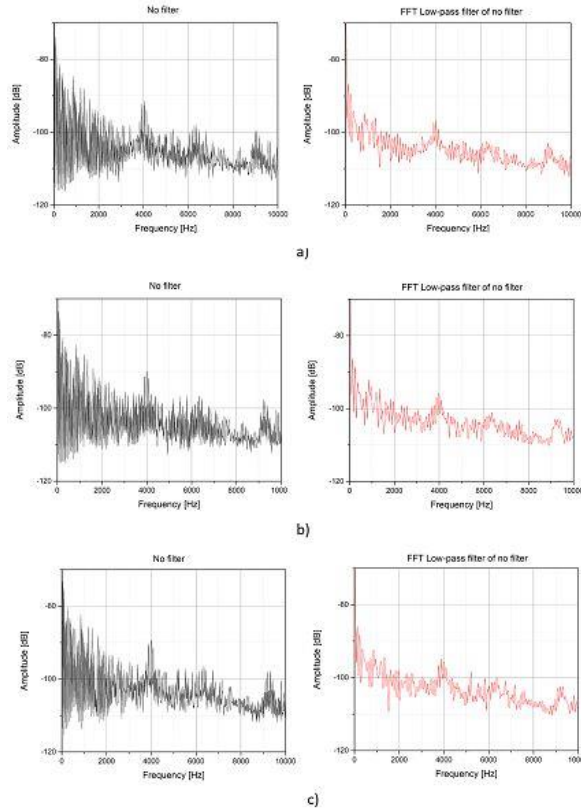


Figure 7 FRF without filters a) 5mm/s; b) 10mm/s; c) 20mm/s

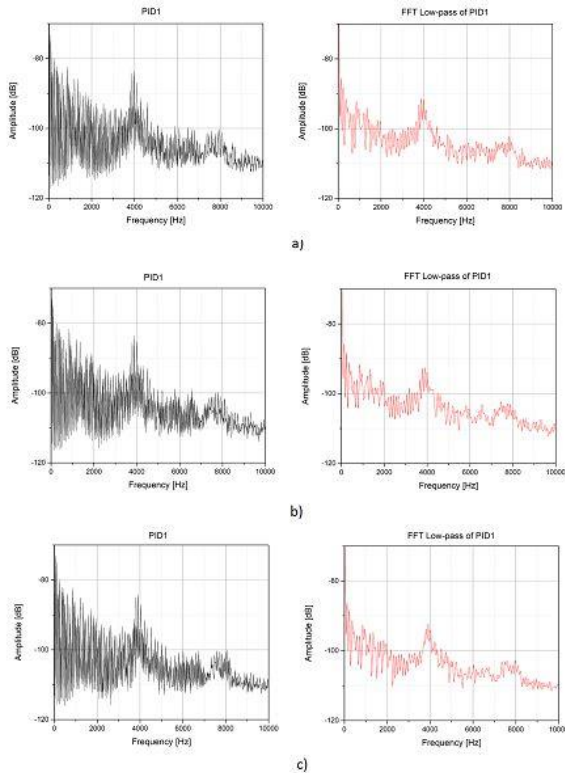


Figure 8 FRF with applied PID1 a) 5mm/s; b) 10mm/s; c) 20mm/s

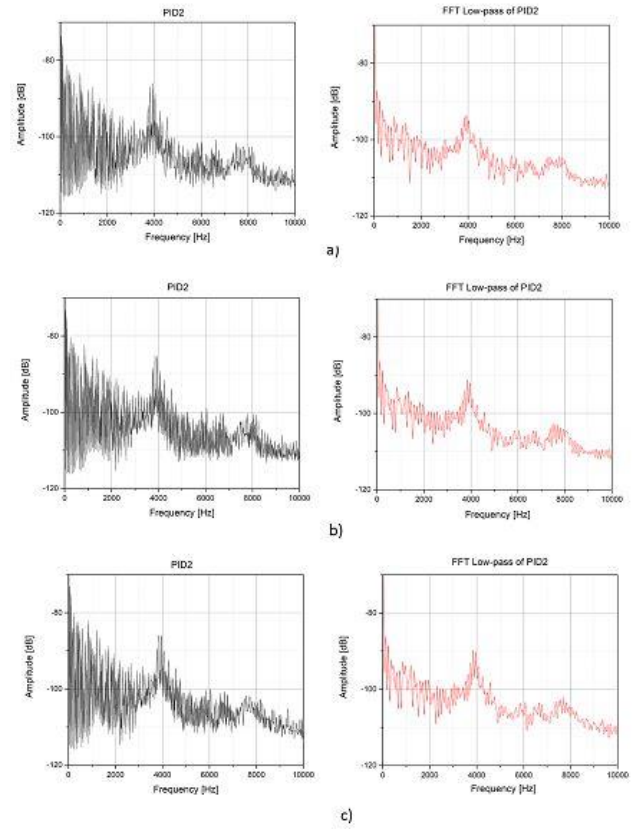


Figure 9 FRF with applied PID2 a) 5mm/s; b) 10mm/s; c) 20mm/s

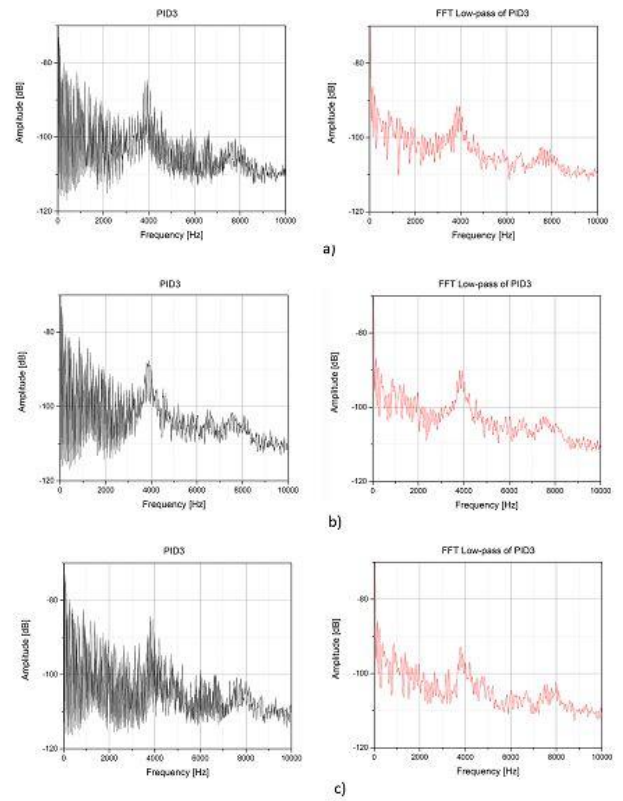


Figure 10 FRF with applied PID3 a) 5mm/s; b) 10mm/s; c) 20mm/s

Analyzed data shows, that highest amplitudes occur at low frequencies. PID3 controller produce positive results at 10mm/s velocity, by reducing amplitudes significantly. PID2 controller produced minimal improvement at 20mm/s. PID1 controller produced negative results at all researched velocities due to observed increase in frequency amplitudes at all frequencies.

All graphs show spike at 4kHz, which occurs due to linear stage construction.

Conclusions

In this paper, experimental research of dynamic processes of the precision positioning system with linear motor based on frequency domain was analyzed by creating experimental setup and using FRF, which showed PID controllers of different architectures effects on the system.

It was observed, that system produced amplitude spike at 4kHz, no matter what kind of controller was used, due to linear stage construction.

To achieve higher stability and lower noise of the system, PID2 controller architecture should be used at higher speeds, and PID3 controller should be used at lower speeds.

References

1. K. Sato and T. Hama, "High-speed positioning of ultrahigh-acceleration and high-velocity linear synchronous motor," *Int. J. Precis. Eng. Manuf.*, vol. 15, no. 8, pp. 1537–1544, 2014, doi: 10.1007/s12541-014-0502-y.
2. M. Salman, "Analysis, design and control aspects of linear machines using co-simulation," 2012.
3. J. Rigelsford, "Linear Synchronous Motors: Transportation and Automation Systems," *Assem. Autom.*, vol. 20, no. 3, p. 3, 2000, doi: 10.1108/aa.2000.03320cad.017.
4. K. M. Tao, R. L. Kosut, and G. Aral, "Learning feedforward control," *Proc. Am. Control Conf.*, vol. 3, no. 3, pp. 2575–2579, 1994, doi: 10.1109/acc.1994.735024.
5. Z. Chen, B. Yao, and Q. Wang, "μ-synthesis-based adaptive robust control of linear motor driven stages with high-frequency dynamics: A case study," *IEEE/ASME Trans. Mechatronics*, vol. 20, no. 3, pp. 1482–1490, 2015, doi: 10.1109/TMECH.2014.2369454.
6. http://www.standa.lt/products/catalog/motorised_positioners?item=667 [Interactive: 2021-04-22].
7. Pišcalov, E. Urbonas, N. Višniakov, D. Zabulionis, and A. Kilikevičius, "Investigation of position and velocity stability of the nanometer resolution linear motor stage with air bearings by shaping of controller transfer function," *Symmetry (Basel)*, vol. 12, no. 12, pp. 1–16, 2020, doi: 10.3390/sym12122062.
8. H. Shim, M. Kochem, and M. Tomizuka, "Use of accelerometer for precision motion control of linear motor driven positioning system," *IECON Proc. (Industrial Electron. Conf.)*, vol. 4, pp. 2409–2414, 1998, doi: 10.1109/iecon.1998.724102.
9. Y. Zeqing, L. Libing, W. Zuojie, C. Yingshu, and X. Quanyang, "Static and Dynamic Characteristic Simulation of Feed System Driven by Linear Motor in High Speed Computer Numerical Control Lathe," *TELKOMNIKA Indones. J. Electr. Eng.*, vol. 11, no. 7, pp. 3673–3683, 2013, doi: 10.11591/telkomnika.v11i7.2813.